Pain 120 (2006) 244–266

PAIN

www.elsevier.com/locate/pain

Pathologic alterations of cutaneous innervation and vasculature in affected limbs from patients with complex regional pain syndrome

Phillip J. Albrecht [a], Scott Hines [b], Elon Eisenberg [c,d], Dorit Pud [e], Deborah R. Finlay [f], M. Kari Connolly [f], Michel Paré [a,1], Gudarz Davar [g], Frank L. Rice [a,*,2]

[a] *Center for Neuropharmacology and Neuroscience, Albany Medical College, Albany, NY, USA*
[b] *Medical School Program, Albany Medical College, Albany, NY, USA*
[c] *Pain Relief Unit, Rambam Medical Center, Haifa, Israel*
[d] *Faculty of Medicine, Technion-Israel Institute of Technology, Haifa, Israel*
[e] *Faculty of Social Welfare and Health Studies, University of Haifa, Haifa, Israel*
[f] *Department of Dermatology, University of California, San Francisco, CA, USA*
[g] *Early Development, Medical Sciences, Amgen, Inc., Thousand Oaks, CA, USA*

Received 15 April 2005; received in revised form 28 September 2005; accepted 13 October 2005

Abstract

Complex regional pain syndromes (CRPS, type I and type II) are devastating conditions that can occur following soft tissue (CRPS type I) or nerve (CRPS type II) injury. CRPS type I, also known as reflex sympathetic dystrophy, presents in patients lacking a well-defined nerve lesion, and has been questioned as to whether or not it is a true neuropathic condition with an organic basis. As described here, glabrous and hairy skin samples from the amputated upper and lower extremity from two CRPS type I diagnosed patients were processed for double-label immunofluorescence using a battery of antibodies directed against neural-related proteins and mediators of nociceptive sensory function. In CRPS affected skin, several neuropathologic alterations were detected, including: (1) the presence of numerous abnormal thin caliber NF-positive/MBP-negative axons innervating hair follicles; (2) a decrease in epidermal, sweat gland, and vascular innervation; (3) a loss of CGRP expression on remaining innervation to vasculature and sweat glands; (4) an inappropriate expression of NPY on innervation to superficial arterioles and sweat glands; and (5) a loss of vascular endothelial integrity and extraordinary vascular hypertrophy. The results are evidence of widespread cutaneous neuropathologic changes. Importantly, in these CRPS type I patients, the myriad of clinical symptoms observed had detectable neuropathologic correlates.

Keywords: RSD; Neuropathic pain; Immunohistochemistry

1. Introduction

Complex regional pain syndromes (CRPS[3] type I or type II, formerly RSD and Causalgia, respectively) are characterized by region specific, spontaneous, chronic pain which develops following a variety of traumas and/or procedures (Raja and Grabow, 2002; Rho et al., 2002; Schwartzman and Popescu, 2002; Jänig

* Corresponding author. Tel.: +1 518 262 5384; fax: +1 518 262 5799.
E-mail address: ricef@mail.amc.edu (F.L. Rice).
[1] Present address: AstraZeneca R&D Montreal, Montreal QC H4S 1Z9, Canada.
[2] Supported in part by: USPHS CA80153, NS34692.
[3] *Abbreviations used:* CRPS, complex regional pain syndrome; FNE, free nerve endings; DRG, dorsal root ganglia; AVS, arteriovenous shunts; PGP, protein gene product 9.5; CGRP, calcitonin gene-related peptide; NF, 200 kDa neurofilament; MBP, myelin basic protein; NPY, neuropeptide Y; TH, tyrosine hydroxylase; DβH, dopamine beta hydroxylase; SP, substance P; VIP, vasoactive intestinal peptide; GAP43, growth associated protein 43; PECAM, platelet/endothelial cell adhesion marker; TRPV1, transient receptor potential vanilloid 1; a2C, alpha 2C adrenergic receptor.

0304-3959/$20.00
doi:10.1016/j.pain.2005.10.035

and Baron, 2003; Kirkpatrick, 2003; Stanton-Hicks, 2003). The clinical features of each type of CRPS are identical, the only diagnostic difference being that a well-defined nerve lesion is present in CRPS type II (causalgia), whereas no identifiable nerve trauma is present in CRPS type I (RSD), calling into question whether or not CRPS type I is a true neuropathic condition (Stanton-Hicks et al., 1995; Wasner et al., 1998; Jänig and Baron, 2003). Most patients diagnosed with CRPS type I have experienced an inciting injury, such as an identifiable soft tissue trauma, a period of immobilization, or an invasive procedure (e.g., surgery or venipuncture), though this injury may range from severe to being so slight that the patient does not recall the incident, and the development or extent of CPRS type I does not depend on the severity of the initiating injury (Galer et al., 2001; Raja and Grabow, 2002; Rho et al., 2002; Schwartzman and Popescu, 2002; Jänig and Baron, 2003; Kirkpatrick, 2003; Stanton-Hicks, 2003).

Clinical features of CRPS may include a mix of sensory, autonomic, and motor symptoms, particularly intractable pain, limb edema, blood flow and sudomotor changes, cutaneous trophic irregularities, and movement disorders (Galer et al., 2001; Raja and Grabow, 2002; Rho et al., 2002; Jänig and Baron, 2003; Kirkpatrick, 2003). CRPS associated pain is described as severe and constant, with deep aching, shooting, and burning sensations. Minor stimulations (e.g., light breeze, clothing on the skin), environmental impacts (e.g., cold, humidity, and pressure), and emotional factors (e.g., anxiety, stress) often exacerbate CRPS pain (Wasner et al., 1998; Galer et al., 2001; Raja and Grabow, 2002; Rho et al., 2002; Kirkpatrick, 2003). Although little histological data exist documenting peripheral neural alterations in CRPS type I affected limbs, abnormal sympathetic (vasomotor, sudomotor) function likely results in the edema and skin discolorations, the range from increased sweating to extremely dry and scaly skin, and the changes in skin, hair, and nail growth patterns (Galer et al., 2001; Raja and Grabow, 2002; Rho et al., 2002; Kirkpatrick, 2003).

Currently, the etiology and underlying pathologic mechanisms responsible for the debilitating pain of CRPS type I are unknown, although peripheral, autonomic, and central nervous system functional alterations are likely involved (Galer et al., 2001; Raja and Grabow, 2002; Jänig and Baron, 2003; Eisenberg et al., 2005). In this investigation of extensive skin samples from two CRPS type I diagnosed patients, we have identified several pathologic changes in cutaneous innervation and vasculature, indicating the presence of peripheral neuropathic conditions that presumably contributed to the clinical symptoms and pathophysiology observed in these two patients.

2. Materials and methods

2.1. Tissue

Human tissue was obtained from surgically amputated extremities from two patients diagnosed with CRPS type I at the Pain Relief Unit at the Rambam Medical Center. One patient required amputation of an upper extremity, the other a lower extremity (Fig. 1). For both CRPS patients, numerous skin samples were taken from several sites immediately following amputation (Fig. 2). The Rambam Medical Center Ethics Committee approved the protocol of sampling tissue for research purposes and both patients provided written informed consent prior to amputation. Control human forearm and palm skin was taken from 5 volunteers at the University of California, San Francisco, Department of Medicine, under the direction of Dr. M. Kari Connolly, and all subjects signed consent forms approved by the UCSF Committee on Human Research. Additional control human finger skin was assessed from an earlier study (Paré et al., 2003).

The upper extremity CRPS patient was a 43-year-old male who sustained a work-related injury to the right shoulder, resulting in a rotator cuff tear, one year prior to his referral to the Pain Relief Unit at the Rambam Medical Center. The shoulder had been placed in a cast for several weeks beginning shortly after the injury and about four months later the rotator cuff and acromio-clavicular joint were surgically repaired. Upon referral to the Pain Relief Unit, the patient complained of intense pain in his right hand and forearm, which was associated with feelings of ''coldness'' and ''numbness'' in the affected hand. On examination, the entire extremity was swollen and wet, and had a red-purple color. Pulses were intact, and the hand was cold (a 4 °C difference between the hands was noted). Light touch and pinprick sensations were increased in the entire hand and the forearm (allodynia and hyperalgesia, respectively). Motor power and range of motion were reduced in the entire extremity. The diagnosis of CRPS type I was made. The patient was treated with various analgesic medications, which included non-steroidal anti-inflammatory agents (diclofenac 100 mg/day; naproxen 100 mg/day), tricyclic antidepressants (amitriptylin 150 mg/day), physical therapy, and repeated axillary and suprascapular nerve blocks with local anesthetics (bupivacain 0.25%, 5–20 ml). A permanent cervical spinal cord stimulator (SCS) was implanted in May 2001 and opioid treatment was initiated. However, the intensity of the pain increased and the hand became even more swollen, totally immobile, and sensitive to touch (Fig. 1A). An amputation through the humerus was performed in April 2002. Large biopsies were harvested from three sites for evaluation (Fig. 2A): transitional glabrous-to-hairy skin from the ventral medial forearm (VMF), glabrous skin from the palmar hypothenar compartment (PHC), and transitional and hairy skin from the dorsal index (2nd) digit (D2D). These sites are innervated by the following dorsal root ganglia and nerves: (1) VMF: C8 and T1 DRGs through the medial antebrachial cutaneous nerve from the medial cord of the brachial plexus; (2) PHC: C8 DRG through the palmar cutaneous branch of the ulnar nerve from the medial cord; (3) D2F: C6 DRG through dorsal digital nerves of the radial nerve from the posterior cord. On patient follow-up, although full recovery of the surgical wound was noted, the patient complained of severe

Fig. 1. Upper and lower extremity of CRPS type I diagnosed patients prior to amputation. The dramatic external changes are clearly visible in the limbs of two CRPS type I diagnosed patients prior to having amputations of the upper (A) or lower (B) extremity as a last resort for pain relief.

squeezing phantom pain immediately after the amputation, and has ongoing burning pain, marked allodynia, and redness in the shoulder, all of which have not yet resolved.

The lower extremity patient was a 45-year-old male who was injured in a car accident in 1997 and sustained a fracture in the first right toe. He received conservative analgesic treatment for over 2 years. In February 2000, an arthrodesis of the 1st metatarso-phalangeal joint was performed. The patient's pain complaints persisted. An electrophysiological study of the feet in May 2000 was negative. Physical examination in June 2000 revealed a dark appearance, reduced ankle and toe range of motion, and tenderness on palpation of the foot. The patient was unable to bear weight on his right foot. Upon examination at the Pain Relief Unit later that year, he had "burning" and "pulling" pain, which he rated as 8 (on a 0–10 numerical pain scale). His foot was not swollen, but had a brown appearance up to the level of the malleoli, with trophic changes of the skin (Fig. 1B). Skin temperature in the affected foot was 2 °C lower than in the healthy one. Ankle and toe motion was restricted. Light touch (allodynia) and pinprick (hyperalgesia) sensations were increased in the entire dorsum of the foot and toes. A diagnosis of CRPS type I was made and he was treated with continuous epidural block with local anesthetics (bupivacain 0.25%, 6–8 ml/h for five days) in September 2000, and later with opioids (oxycodone 60 mg/day), NSAIDs (naproxen 100 mg/day; rofecoxib up to 50 mg/day), and antidepressants (clomipramine 75 mg/day) for nearly two years with only minimal improvement. On repeated examination, light touch (allodynia) and pinprick (hyperalgesia) sensations were suspected to be slightly more intense in the lateral aspect of the foot, in the territory of one of the branches of the superficial peroneal nerve (SPN). The SPN was transected and buried in bone. As no relief was obtained subsequent to this procedure, a spinal cord stimulator trial was performed in May 2002. This was also unsuccessful so no permanent implantation took place. Finally, the leg was amputated below the knee in September 2002. Four biopsy sites were evaluated where pain threshold testing had been performed (Fig. 2B). Two sites had severe pain sensation: transitional glabrous-to-hairy skin from dorsal lateral foot (DLF) and transitional and hairy skin from the dorsal second toe (D2T). Two areas had a relatively normal sensation: hairy skin from the dorsal lateral leg (DLL) and glabrous skin from the lateral plantar compartment (LPC). These sites are innervated by the following dorsal root ganglia and nerves: (1) DLF: S1, S2 DRGs through the sural nerve derived from the tibial and common peroneal nerve; (2) D2T (medial half): L4, L5 DRGs through dorsal digital nerves from the deep peroneal nerve; (3) DLL: L5, S1 DRGs through the lateral sural cutaneous nerve from the common peroneal nerve; (4) LPC: L5, S1 DRGs through the plantar cutaneous branches of the lateral plantar nerve from the tibial nerve. These four sites are not normally innervated by the superficial peroneal nerve which was transected, with the exception of the lateral half of D2T which should normally be innervated by a dorsal digital nerve derived from the superficial peroneal nerve. On patient follow-up, it was noted that subsequent to the amputation the patient reported partial pain relief for a short period. However, a few weeks later he began feeling severe stump pain and mild to moderate phantom

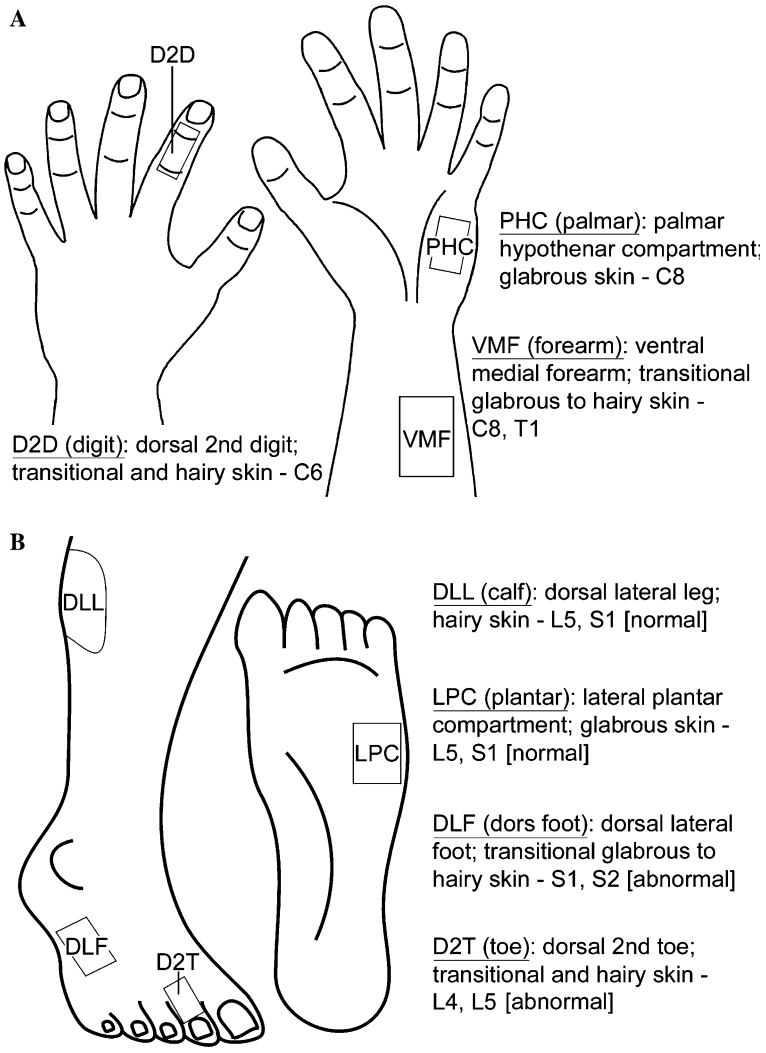

Fig. 2. Depictions of the CRPS upper and lower extremity skin areas evaluated. Skin samples were taken from several areas of the amputated upper (A) and lower (B) extremity of two patients diagnosed with CRPS type I. Anatomical areas are defined and include the labels used in the figures to represent each region (in parentheses), the type of skin from each region, and the level of the DRG/spinal nerves that provide innervation to each region. Additionally, pain threshold testing was performed on the lower extremity patient prior to amputation, and based upon the test results, each region was determined to be normal (CRPS uninvolved skin) or abnormal (CRPS involved skin).

sensation. Medical treatment with carbamazepine, oxycodone, and intravenous ketamine and lidocaine infusions was not helpful. In October 2004, a surgical removal of neuromas from the common peroneal, sural, and tibial nerves was performed, however the patient still experiences stump pain.

From each of the CRPS biopsy sites, the skin was sliced into 3–5 strips approximately 1 cm long and 3 mm wide, oriented parallel to the long axis of the extremity. Skin from palm and forearm of control volunteers consisted of 5 mm punch biopsies. The strips and punch biopsies were fixed overnight by immersion in 4% paraformaldehyde in 0.1 M phosphate-buffered saline (pH 7.5) at 4 °C. Following fixation, the skin was rinsed, stored in cold PBS with 0.1% NaN_3, and shipped overnight to Albany Medical College for processing. Tissue to be sectioned was cryoprotected by overnight infiltration with 30% sucrose in PBS and cut by cryostat into 14 μm sections perpendicular to the skin surface and parallel to the long axis of the skin samples. Sections were rotated across a series of 10 slides to allow staining of adjacent sections with various antibodies. The sections were thaw mounted onto chrome-alum-gelatin-coated slides, air-dried overnight, and processed for single or double immunolabeling.

2.2. Immunofluorescence

Immunofluorescence was assessed by single-label and double-label combinations using primary antibodies directed against a battery of antigens associated with innervation and nociceptive processing (Table 1). Slides with sections were pre-incubated in 1% bovine serum albumin and 0.3% Triton X-100 in PBS (PBS-TB) for 30 min and then incubated with primary antibody diluted in PBS-TB overnight in a humid atmosphere at 4 °C. Slides were then rinsed in excess PBS for 30 min and incubated for 2 h at room temperature with the appropriate Cy2-, Cy3-, or Alexa488-conjugated secondary antibodies (Jackson ImmunoResearch, West Grove, PA; Molecular Probes, Eugene, OR) diluted in PBS-TB. Following secondary antibody incubation, the sections were rinsed for 30 min in

Table 1
Antibodies used for immunohistochemical analysis

Antigen[a]	Antibody (dilution)	Source
PGP	Rb poly (1:1000)	UltraClone (Wellow, UK)
CGRP	Sh poly (1:800)	Affiniti Research Products (Exeter, UK)
	Rb poly (1:800)	Chemicon (Temecula, CA)
	Gp poly (1:400)	Peninsula Laboratories (San Carlos, CA)
NF (200 kDa subunit)	Rb poly (1:800)	Chemicon (Temecula, CA)
MBP	Ms mono (1:1000)	Sternberger (Baltimore, MD)
NPY	Sh poly (1:800)	Chemicon (Temecula, CA)
TH	Rb poly (1:800)	Chemicon (Temecula, CA)
DβH	Rb poly (1:800)	Chemicon (Temecula, CA)
SP	Gp poly (1:400)	Research Diagnostics (Flanders, NJ)
VIP	Rb poly (1:2000)	Incstar (Stillwater, MN)
GAP-43	Ms mono (1:1000)	gift of Dr. David J. Schreyer
PECAM	Ms mono (1:50)	DAKO (Glostrop, Denmark)
TRPV1	Gp poly (1:1000)	Neuromics (Northfield, MN)
Alpha 2C (α2C)	Rb poly (1:1000)	Stone et al. (1998)

List of the antibodies, including the dilutions and sources, used for these evaluations.

[a] PGP, protein gene product 9.5; CGRP, calcitonin gene-related peptide; NF, 200 kDa neurofilament; MBP, myelin basic protein; NPY, neuropeptide Y; TH, tyrosine hydroxylase; DβH, dopamine beta hydroxylase; SP, substance P; VIP, vasoactive intestinal peptide; GAP43, growth associated protein 43; PECAM, platelet/endothelial cell adhesion marker; TRPV1, transient receptor potential vanilloid 1; α2C, alpha 2C adrenergic receptor.

PBS and either processed for a second round of primary and secondary antibodies or coverslipped under 90% glycerol in PBS. Additionally, following the secondary antibody rinses, some slides were counterstained with the nuclear dye Hoechst prior to coverslipping. When the pairs of primary and secondary antibodies used for a specific double label combination were raised in different species that did not cross label, the double label immunostaining was carried out in cocktailed mixtures of primary antibodies, followed by cocktailed mixtures of secondary antibodies using the same procedures as above. Alternatively, double labeling was conducted sequentially doing a first round with one type of primary antibody followed by an appropriate Cy3-conjugated secondary antibody, then a second round with a different primary antibody followed by a Cy2 or Alexa488-conjugated secondary antibody. Under certain circumstances, using sequential immunostaining rounds to achieve double labeling can be done even if the first and second primary antibodies are identical species raised polyclonals (see Rice et al., 1997). Controls for the specificity of the antibodies had been assessed in prior studies of rodent, human, and primate skin (Rice et al., 1997; Paré et al., 2001; Petersen et al., 2002). Throughout the text we describe each specific antibody label by simply referring to the antigenic marker (e.g., NF-positive, NF staining, NF labeling, fibers express NF, and fibers labeled with NF), and in every case these references recognize the concept that the staining is of anti-NF200 antibodies, for example, and that this type of immunolabeling is also commonly referred to as immuno-like reactivity (IR), as in NF-IR, for example.

2.3. Analysis

Immunostained sections were analyzed with an Olympus Optical Provis AX70 microscope equipped with conventional fluorescence filters (Cy3: 528–553 nm excitation, 590–650 nm emission; Cy2/Alexa488: 460–500 nm excitation, 510–560 nm emission; DAPI/Hoechst: 375–400 nm excitation, 450–475 emission). Fluorescent images were collected with a high-resolution camera (Sony, DKC-ST5) interfaced with Northern Eclipse (Empix Imaging, Mississaugau, ON), Photoshop (Adobe, San Jose, CA), and NeuroLucida (MicroBrightField, Colchester, VT) software. Procedures for capturing the images, analyzing for double labeling, and modifying images for purposes of published documentation are described in detail in Paré et al. (2001). PGP-positive and CGRP-positive epidermal endings were quantified from three sections each from control and CRPS affected regions using the NeuroLucida/Neuroexplorer software application to mark endings and measure epidermal lengths. Data are presented as means and standard errors of three independent counts, and comparisons between control and CRPS affected skin regions were performed utilizing Student's *t*-test. Vascular and sweat gland innervation quantification consisted of evaluating a total of 20 vessels and 20 sweat glands each from randomly selected sections of control or CRPS affected skin regions and determining if CGRP-positive innervation was present or absent. Data are presented as the number of vessel and sweat gland profiles that received CGRP-positive innervation from the 20 sampled. A two-tailed Fishers Exact test was used to determine whether there was a significant difference between the controls and CRPS affected skin regions.

3. Results

Immunohistochemical analysis of both upper and lower extremity CRPS skin biopsies revealed morphological and biochemical alterations in cutaneous innervation and vasculature within the affected skin as compared with biopsies from the forearm and hand of normal control subjects or from non-painful "control" sites on the amputated lower extremity. Variability in innervation quality and density was often present within sections from the same biopsy, including controls, over a distance that spanned at least 5 mm and up to 10 mm of skin surface. The immunofluorescence images presented are representative of the typical control and pathological innervation, as well as additional unusual deviations that were not seen in control human skin in this study, or in extensive evaluations of control skin in previous and ongoing studies that have involved 3 mm punch biopsies of thoracic skin in 95 human subjects, entire fingers from 3 human subjects, 5 mm punch biopsies from the palms and forearms of 5 human subjects, and entire hands of 15 macaque monkeys (Paré et al., 2001, 2002, 2003; Petersen et al., 2002).

Abnormalities that were detected in the upper and lower extremity CRPS affected skin included: (1) a reduction or absence of thin caliber axons that co-ex-

press NF and MBP, indicative of normal Aδ fibers, and the abnormal presence of numerous thin-caliber NF-positive axons that lacked MBP labeling (Figs. 3 and 4); (2) a reduction of epidermal and upper dermal innervation supplied by C fibers and Aδ fibers (Figs. 5, 6, and 14) and a concomitant abnormal dense plexus of thin caliber innervation around hair follicles (Fig. 7); (3) a disruption of Aβ fiber Meissner corpuscle, Merkel cell, and lanceolate hair follicle innervation (Figs. 5–7); (4) aberrant sweat gland innervation that included a loss of normal CGRP-positive innervation, and the presence of aberrant NPY and DβH-positive innervation (Figs. 8, 9, and 14); and (5) disruptions in vascular innervation and structure (Figs. 10–14).

3.1. Fiber types in cutaneous nerves

Cutaneous nerves in the dermis from control forearm and palmar skin (Figs. 3 and 4) contained a mix of large and small caliber fibers that labeled with NF (Figs. 3B, C, H, and I). Virtually all of these NF-positive fibers co-labeled with MBP (Figs. 3A–C), indicating that they are large-caliber Aβ and small-caliber Aδ fibers. Presumptive Aβ fibers have been shown to terminate as morphologically distinct varieties of Merkel, Meissner, Pacinian, and lanceolate endings associated with low threshold, high conduction rate mechanoreceptors, whereas Aδ fibers terminate in the epidermis, in the tunica adventitia of blood vessels, and around hair follicles as free nerve endings (FNE) that lack distinct morphological specializations. In normal nerves, NF-positive axons are interspersed among gaps occupied by bundles of likely C fibers that typically lack NF and MBP, and that terminate predominantly in the epidermis and around blood vessels and hair follicles as FNE (Figs. Figs. 5–10; Fundin et al., 1997a,b; Rice et al., 1997; Rice and Rasmusson, 2000; Paré et al., 2001, 2002; Fünfschilling et al., 2004). As seen in NF labeled preparations (Figs. 3A–C, G–I), the control nerves displayed these gaps between the NF/MBP-positive axons that are filled with bundles of numerous NF/MBP-negative small caliber unmyelinated C-fibers (as seen in PGP labeled nerves). Most of these presumptive C fibers had detectable GAP43, which was not present in control Aβ and Aδ fibers (Figs. 3G–I). As shown in CRPS forearm skin (Figs. 3D–F, J–L), the cutaneous nerves contained some normal looking large caliber Aβ fibers that co-express NF and MBP, and lack GAP43, as in control skin. However, in contrast to nerves in control skin, nerves from CRPS skin had no small caliber Aδ fibers that clearly co-expressed NF and MBP. Instead, the nerves were packed with numerous bundles of thin axons that expressed NF without MBP (Figs. 3D–F), indicating the absence of myelin on these thin NF-positive fibers. Furthermore, these aberrant NF-positive/MBP-negative thin caliber axons mostly lacked GAP43. However, GAP43 was still present in bundles of small caliber presumptive C fibers that remained NF-negative (Figs. 3J–L).

Previous studies have shown that subsets of normal Aβ, Aδ, and C fibers label for CGRP and SP, whereas other Aβ, Aδ, and C fibers lack detectable CGRP or SP (Fundin et al., 1997a,b; Rice et al., 1997; Rice and Rasmusson, 2000; Fünfschilling et al., 2004). In both control and CRPS skin, numerous thin caliber CGRP-positive axons were present in nerves located in the deep dermis at or below the level of Pacinian corpuscles (Fig. 4). In control skin, many CGRP axons continued through more superficial nerves to innervate the epidermis, as well as hair follicles, sweat glands, and blood vessels in the upper dermis (Figs. 5G; 8C; 10E; Table 2). In contrast, significantly less CGRP-positive innervation was detected at these more superficial levels in CRPS skin (Figs. 5H; 8G, K, O; 10F; Table 2).

Interestingly, most of the CGRP-positive fibers in the deep nerves of the CRPS skin also co-expressed the TRPV1 receptor (Figs. 4D–F), whereas TRPV1 is not usually detected in CGRP-positive innervation in control primate and human skin (Paré et al., 2001; Petersen et al., 2002). Additionally, as is also seen in control tissues, some double labeling revealed that CGRP-positive processes typically co-expressed substance-P (SP), but no processes expressed SP without CGRP.

3.2. Upper dermal and epidermal innervation

Although GAP43-positive C fibers are abundant in deep and superficial nerves in both control and CRPS skin (Figs. 3G–I, J–L), significantly fewer fibers appear to innervate the upper dermis and epidermis in CRPS as compared to control skin (Table 2). In contrast to the numerous epidermal endings consistently seen in control forearm, palmar, and digital skin (Figs. 5A, C, and E), comparable CRPS affected skin had a marked reduction of epidermal innervation (Figs. 5B, D, and F; Table 2). Consistent with the reduction of endings in the epidermis, the upper dermis and dermal papillae in CRPS skin had few detectable nerves and thin-caliber axons, which are the C and Aδ fiber sources of the epidermal innervation, as compared to control skin (Figs. 5A–F). Likewise, lower extremity CRPS skin, including involved and uninvolved regions, also had apparent losses of epidermal and upper dermal innervation (Figs. 14A, D, H, and K). Interestingly, no Aβ-fiber Meissner or Merkel endings were detected in the glabrous foot skin samples, an area indicated as having normal pain thresholds. Losses of epidermal innervation density have consistently been shown in other neuropathic conditions, however, the loss of epidermal innervation, per se, does not directly lead to a painful disease condition (FL Rice, unpublished observation; see also Rowbotham and Fields, 1996; Holland et al., 1997; Oaklander, 2001; Petersen et al., 2002). Therefore, these presumed

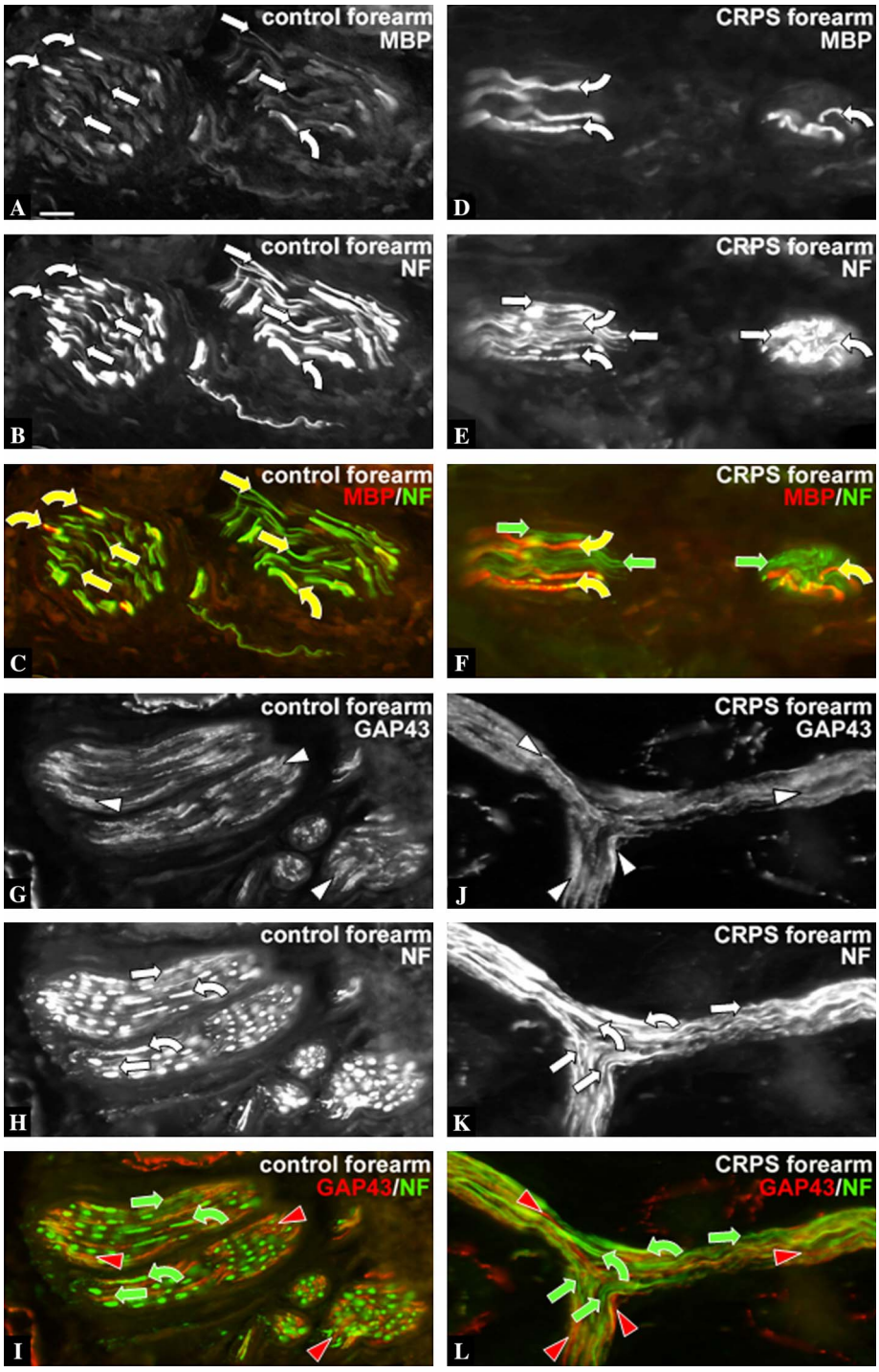

Fig. 3. Nerves from CRPS forearm skin lacked normal Aδ fibers but have aberrant thin caliber NF-positive fibers. Images are of nerves at comparable mid-dermal levels, superficial to the location of Pacinian corpuscles. Each set of three panels depicts the single- and double-labeled images for the antigens indicated in the upper right corners. The first and second grayscale images in each set show the labeling obtained with red and green fluorescent secondary antibodies, respectively. The third image shows the combined color images with single-labeled components indicated with red or green symbols for the corresponding fluorophore, and double-labeled components indicated by yellow symbols. (A–F) In control nerves (A–C), NF and MBP were consistently co-expressed revealing a mix of thick NF-positive Aβ fibers that had relatively intense MBP labeling (curved arrows) and thin NF-positive, presumptive Aδ fibers that had relatively weak MBP labeling (arrows). CRPS nerves (D–F) also had large caliber NF and MBP-positive Aβ fibers (curved arrows), but otherwise contained a dense concentration of thin caliber NF-positive fibers that did not have any detectable MBP signal (arrows). Note that the normal nerve had wide immunonegative gaps whereas the CRPS nerve was filled with anti-NF labeling. (G–L) In control nerves (G–I), the gaps between NF-positive axons were packed with bundles of numerous very thin caliber presumptive C fibers, many of which expressed GAP43 (arrowheads). GAP43 is usually lacking in NF-positive axons. In CRPS nerves (J–L), GAP43 expression remained on only a subset of thin caliber fibers and fiber bundles (arrowheads) that remained largely NF-negative. The aberrant small NF-positive fibers were largely GAP43-negative (arrows). Scale bar = 25 μm.

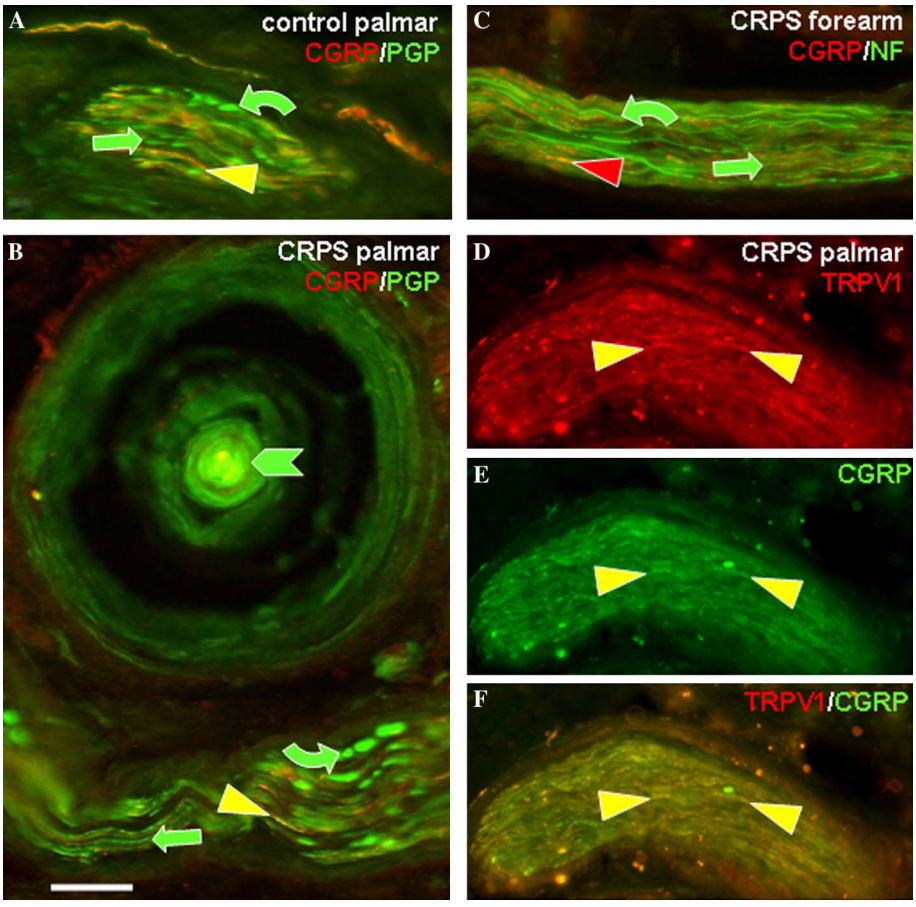

Fig. 4. Deep dermis in CRPS skin had normal appearing Pacinian corpuscles and nerves contained numerous TRPV1/CGRP-positive thin caliber axons. Single and double labeled images are for the antigens indicated in the upper right corners. Single labeled components are indicated with red or green symbols for the corresponding fluorophore, and double labeled components are indicated by yellow symbols. (A,B) Nerves in the deep dermis (i.e., at the level of Pacinian corpuscles) of control and CRPS palmar skin contained a mix of large and small caliber axons that were only labeled with PGP (curved and straight green arrows, respectively), and numerous small caliber axons that also labeled with CGRP (yellow arrowheads). Pacinian corpuscles in the CRPS skin appeared to be normal, with the Aβ fiber ending located at the core (green chevron). (C) As seen in this CRPS forearm section, CGRP was found on small caliber axons (red arrowhead) that lacked NF expression seen on other small caliber fibers (green straight arrow) and large caliber Aβ fibers (green curved arrow). (D–F) Separate single labeled images (D,E) and the corresponding merged image (F) indicated that most of thin caliber fibers labeled with CGRP also co-expressed TRPV1 (yellow arrowheads). Scale bar = 50 μm.

losses of epidermal innervation in both involved and uninvolved regions of the lower extremity patient, although pointing to a loss of small-caliber fibers, cannot be used as a sole explanation for the presence or absence of abnormal pain.

The decrease in epidermal endings and dermal fibers in CRPS skin included a significant depletion of CGRP-positive axons and endings in comparison to control skin (Figs. 5G, H; 12; Table 2), and the little remaining CGRP-positive innervation was typically restricted to dermal papillae and often co-expressed TRPV1 (Figs. 6C and D). Although overall epidermal and upper dermal innervation was generally depleted in CRPS skin, some small focal sites had excessive innervation that included dense NF-positive and -negative innervation (Fig. 6A). In such locations, NF labeling continued abnormally onto endings that penetrated well into the epidermis (Fig. 6A). In control sites and CRPS areas with depleted innervation, NF seen on relatively small caliber axons in the upper dermis and in dermal papillae did not continue onto endings that penetrated the epidermis (Fig. 6B). Among the relatively few endings that did innervate the epidermis in CRPS skin, some had highly branched, extensive arborizations (Fig. 6H), whereas normal epidermal endings are relatively straight and unbranched (Figs. 5A, C, E).

3.3. Glabrous skin Aβ fiber innervations

In glabrous skin, the Aβ fibers normally terminate: (1) in Pacinian corpuscles; (2) in Meissner corpuscles in dermal papillae (Figs. 5C and E), and (3) as endings on Merkel cells in stratum basalis at the base of epidermal ridges (Figs. 5C and E). Consistent with the presence of at least some Aβ fibers in the nerves (Figs. 3D–F, J–L), the CRPS skin did contain a few normal

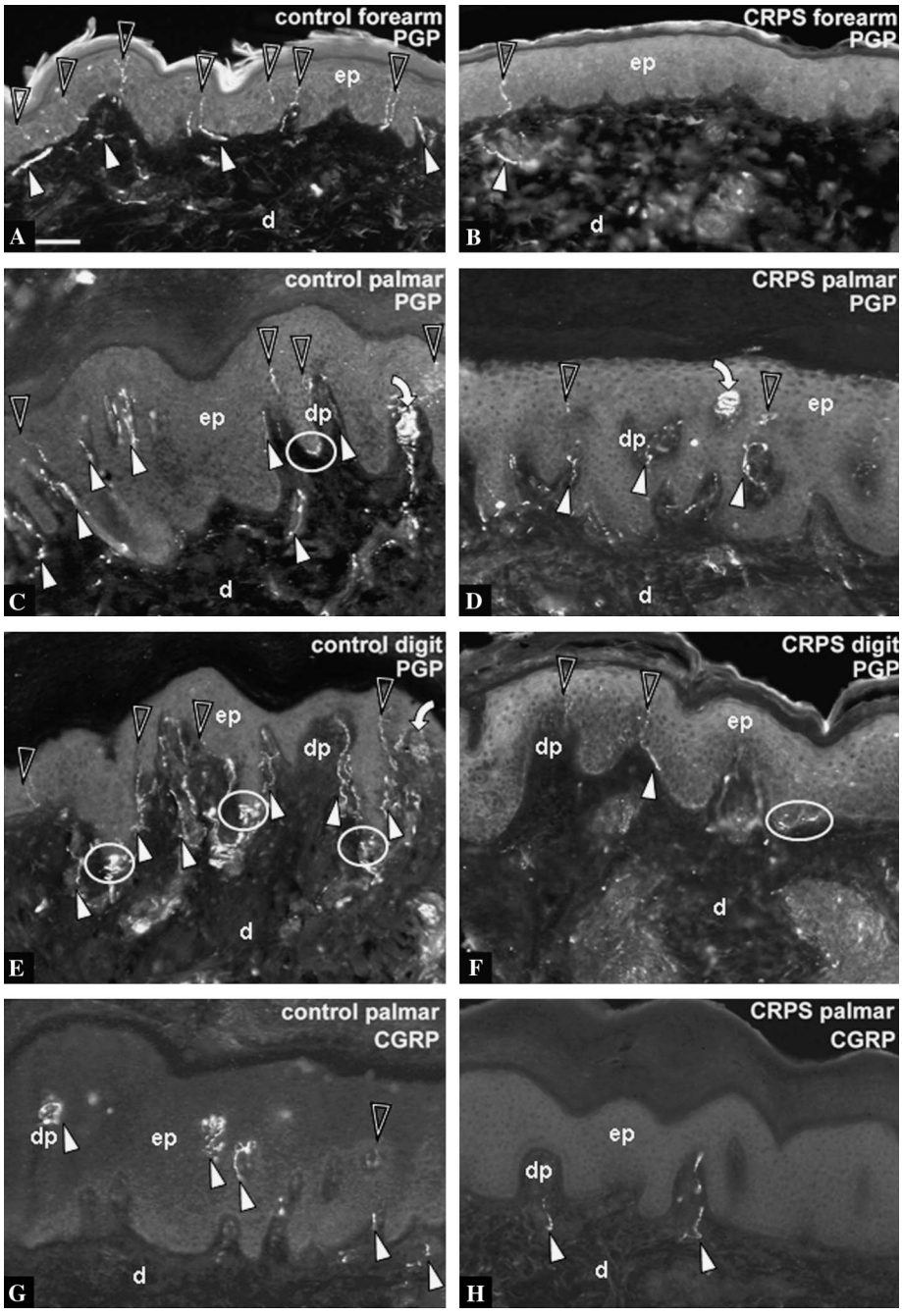

Fig. 5. CRPS upper extremity skin samples lacked epidermal and upper dermal innervation compared with control skin. (A–F) Labeling with PGP revealed that CRPS affected upper extremity skin (B, D, F) had a dramatic loss of FNE in the epidermis (open arrowheads) and small nerves and axons in the upper dermis (solid arrowheads) compared with control skin (A, C, E). Although the CRPS skin still retained some normal looking Meissner corpuscles (curved arrows) and Merkel endings (inside ovals), these Aβ-fiber endings were rarely seen compared with control skin. (G,H) Although deep nerves in CRPS skin contained numerous CGRP-positive axons, in comparison to control skin, hardly any CGRP was detected among the epidermal and upper dermal innervation. d, dermis; dp, dermal papilla; ep, epidermis. Scale bar = 50 μm.

looking Pacinian corpuscles (Fig. 4B), Meissner corpuscles (Figs. 5D and 6G), and Merkel endings (Figs. 5F, 6E, F), however, such normal Meissner corpuscles and Merkel endings were rarely seen. Instead, many dermal papillae that would normally contain Meissner corpuscles had tangles of disorganized NF-positive fibers that may be disrupted corpuscles (Fig. 6A).

3.4. Hair follicle innervation

Innervation to hair follicles in control forearm tissue (Figs. 7A and C) included the termination of NF-positive Aβ fibers and NF-negative C fibers in piloneural complexes that are located around the perimeter of hair follicles, just below the level of the sebaceous gland. The

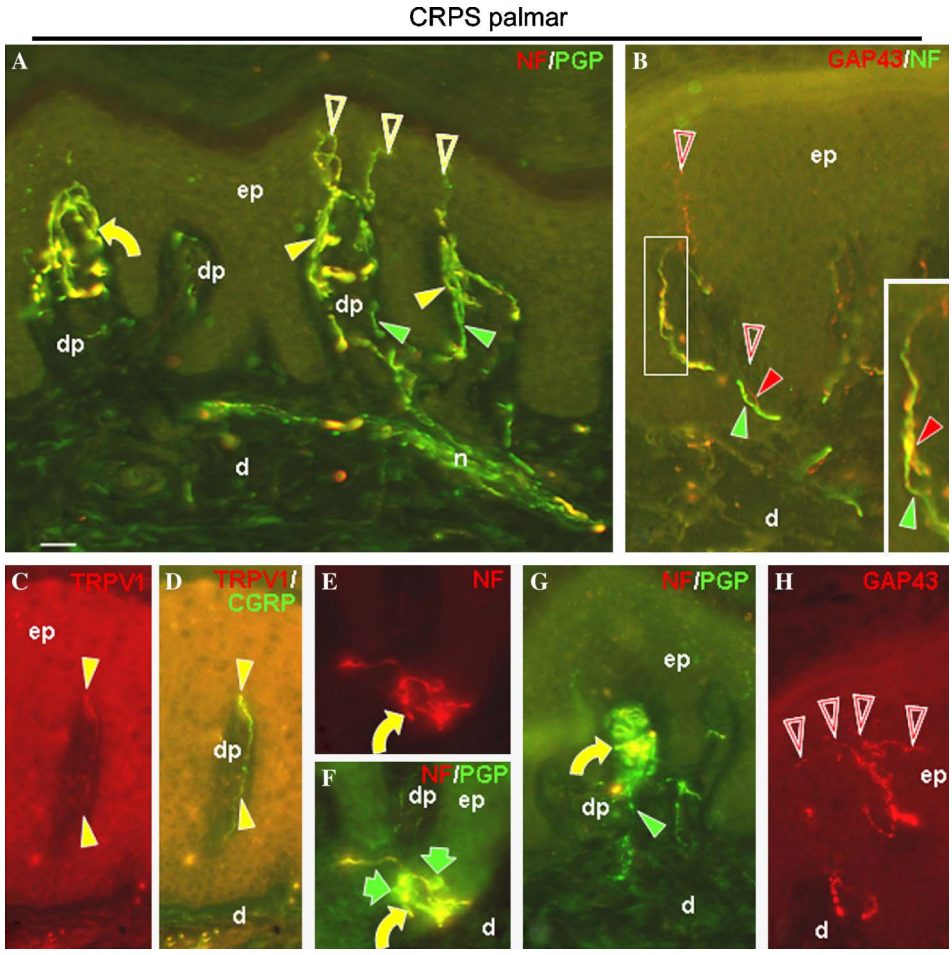

Fig. 6. Examples of different varieties of innervation abnormalities in CRPS palmar skin. (A) Although most sites in the epidermis and upper dermis had reduced innervation in CRPS skin, this small focal site had exceptionally dense NF-positive and NF-negative dermal papilla innervation (yellow and green solid arrowheads, respectively) that included a cluster of NF-positive endings extending abnormally into the epidermis (yellow open arrowheads). The curved arrow indicates a tangle of NF-positive thicker caliber innervation in a dermal papilla that may be a disrupted Meissner corpuscle. (B) Consistent with the normal separation of NF and GAP43 labeling in nerves, this site in CRPS skin had some NF-positive/GAP43-negative fibers which extended into dermal papillae (green solid arrowhead), but did not penetrate the epidermis, while other very thin caliber NF-negative/GAP43-positive dermal fibers (red solid arrowhead) did innervate the epidermis (red open arrowheads). Inset is an enlargement of the area in the white rectangle showing that the NF-positive fiber was closely intertwined with the GAP43 fiber, but both labels were not in the same fiber. (C,D) Consistent with TRPV1/CGRP double labeling in deep nerves, the few CGRP-positive fibers that did extend into dermal papillae co-expressed TRPV1 and CGRP (yellow arrowheads). (E,F) An example of rare Merkel cell innervation in CRPS skin. NF and PGP co-labeled the Aβ fiber and its endings (yellow curved arrow), whereas only PGP labeled the few Merkel cells (green arrows). (G) One of the few normal appearing Meissner corpuscles in CRPS skin that contained both the normal complement of NF-positive Aβ-fiber endings (yellow curved arrow), as well as normal intermingled C-fiber endings (green arrowhead). (H) Although epidermal endings were generally reduced in CRPS skin, remaining C-fiber endings, shown here with GAP43, had an abnormal highly branched terminal arborization (open arrowheads). d, dermis; dp, dermal papilla; ep, epidermis. Scale bar = 25 μm (A–H) and = 12.5 μm (B, inset).

Aβ fibers terminated primarily as palisades of regularly spaced, longitudinally oriented lanceolate endings that lacked GAP43 (Figs. 7A and C). The C fibers commonly expressed GAP43 and terminated in a circumferential orientation centrifugal to the lanceolate palisades (Fig. 7C). Normally, some C-fiber endings are CGRP-positive and others are CGRP-negative (not shown). Although some C fibers and Aδ fibers normally innervate the neck of hair follicles located above the sebaceous glands, little innervation of any kind is normally present around the follicles below the level of the pilo-neural complexes (Figs. 7A and C). In CRPS affected forearm skin, the normally ordered lanceolate endings were highly disorganized and dense abnormal plexuses of thin caliber fibers had ramified below, within, and above the zone of the lanceolate endings (Figs. 7B, D, and E). The thin fibers in these aberrant plexuses were a mix of GAP43-positive/NF-negative fibers and GAP43-negative/NF-positive fibers (Fig. 7D) with aberrant terminations. The numerous small caliber NF-positive fibers that form these aberrant plexuses on hair follicles likely arise from the aberrant small caliber

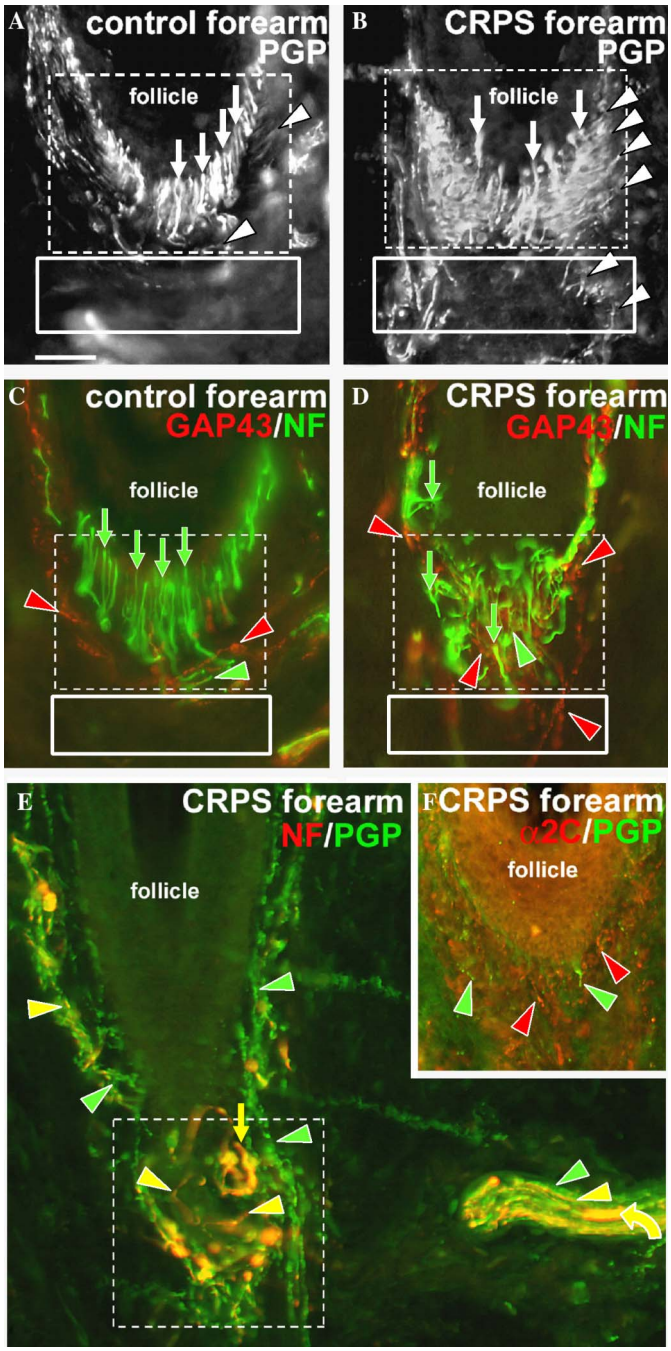

Fig. 7. Hair follicles in CRPS skin had disrupted normal innervation and additional aberrant innervation. (A,C) Control follicles were innervated by piloneural complexes (broken line rectangles) consisting of a palisade of evenly spaced, longitudinally oriented lanceolate endings (arrows) supplied by NF-positive large caliber Aβ fibers, and circumferentially oriented endings (arrowheads) supplied by a mix of GAP43-positive/NF-negative C-fibers (red arrowheads) and GAP43-negative/NF-positive moderate caliber Aβ fibers (green arrowhead). Very little innervation was normally present immediately below (solid line rectangles) or above the piloneural complexes. (B, D–F). In CRPS skin, the piloneural complexes (broken line rectangles) were in disarray with irregularly oriented lanceolate endings (arrows) and dense concentrations of disorganized small fiber terminations (arrowheads). Dense plexuses of small caliber terminations were also in aberrant locations below (B,D, solid line rectangles) and above (E) the piloneural complexes. Consistent with the content of CRPS nerves (E, lower right; also Figs. 3D–F, J–L), the aberrant plexuses of small caliber innervation included GAP43-positive/NF-negative and GAP43-negative/NF-positive fibers. The nerve also contained some Aβ fibers (curved arrow) that are presumably the source of the lanceolate endings. (F) Some fibers contributing to the aberrant plexuses labeled only with α2C (red arrowheads), indicating that PGP may not reveal some abnormal innervation. Scale bar = 25 μm.

NF-positive fibers in the nerves (Fig. 7E; see also Figs. 3F, L). Additionally, we found an abnormal presence of α2C-adrenergic receptors on very thin, disorganized fibers around hair follicles. Surprisingly, this presumptive innervation appears to lack PGP expression (Fig. 7F). The expression of α2C-adrenergic receptors

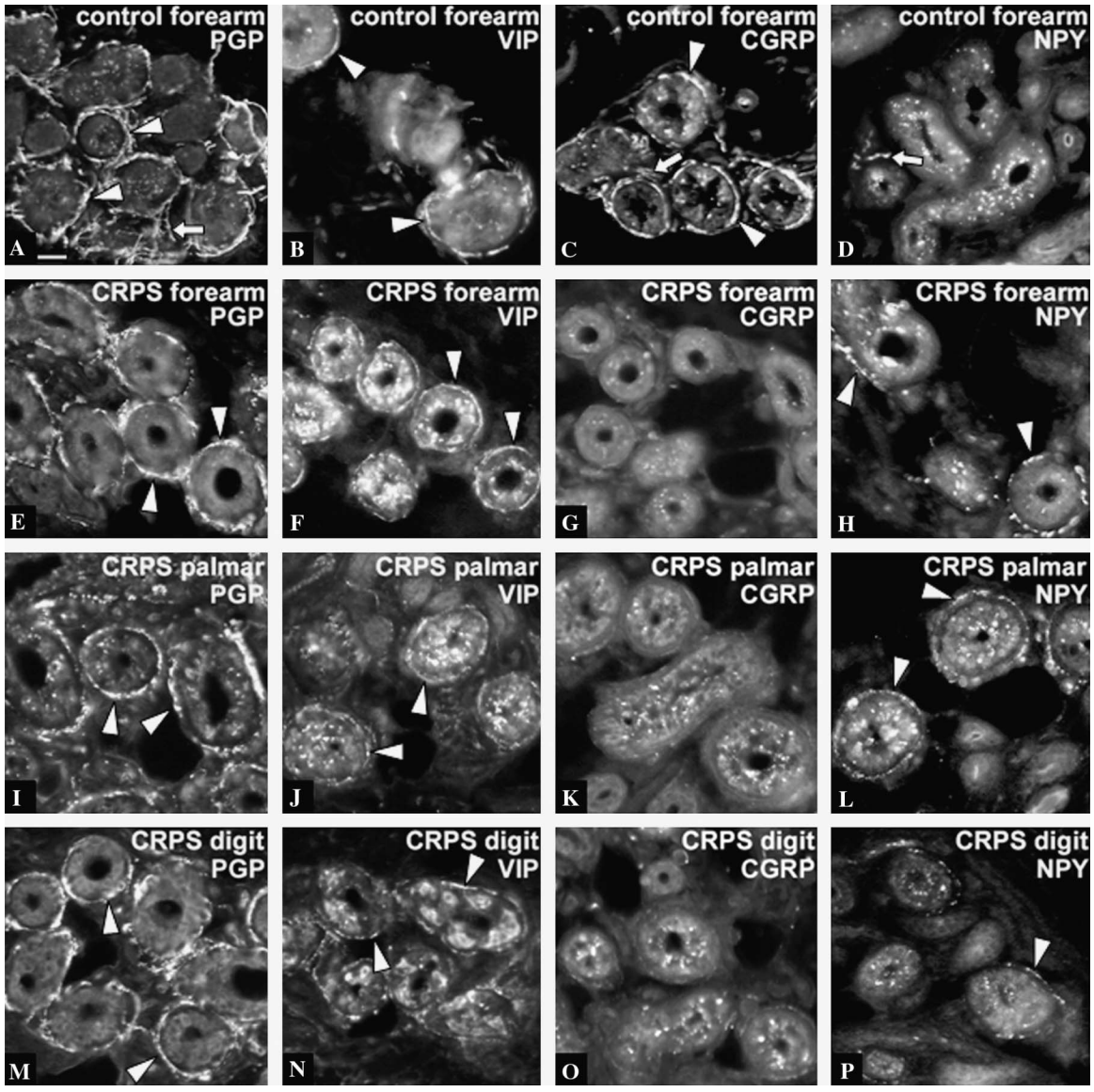

Fig. 8. CRPS affected arm skin innervation to sweat glands usually lacked normal CGRP expression and had aberrant NPY expression compared with control. (A–D) Sweat glands from control forearm biopsies had abundant PGP-positive innervation (A, arrowheads). Most of the innervation contained VIP (B, arrowheads) and a smaller proportion co-expressed CGRP (C, arrowheads). CGRP was also expressed on some fibers accompanying small blood vessels within the sweat glands (C, arrow). NPY was normally only detected on the small blood vessels (D, arrow). (E–P) In contrast, sweat glands from CRPS affected arm skin that had remaining PGP-positive innervation (arrowheads in E, I, and M) contained VIP-positive fibers (arrowheads in F, J, and N), but had lost the normal contingent of CGRP expression (G, K, and O). Furthermore, the affected sweat gland innervation had an abnormal expression of NPY around the sweat gland tubules (arrowheads in H, L, P). Scale bar = 25 μm.

is most commonly associated with presynaptic expression and inhibition of neuronal activity. Therefore, although the levels of circulating catecholamine levels have been shown to be decreased in affected CRPS limbs, the abnormal expression of α2C observed on CRPS hair follicle innervation may represent a compensatory mechanism attempting to abort increased neuronal firing in these fibers where a supersensitivity to sympathetic output has been established (Jänig, 1990; Drummond et al., 1991; Sato and Perl, 1991; Harden et al., 1994).

3.5. Sweat gland innervation

During normal sweat gland development, the sympathetic innervation is originally adrenergic and expresses TH and DβH. However, the interaction with maturing sweat gland tubules causes the adrenergic properties of the innervation to virtually disappear as the fibers gain a cholinergic phenotype (Schotzinger and Landis, 1990). Cholinergic sympathetic fibers that also contain VIP are the predominant innervation to normal mature sweat glands and are typically the only innervation dis-

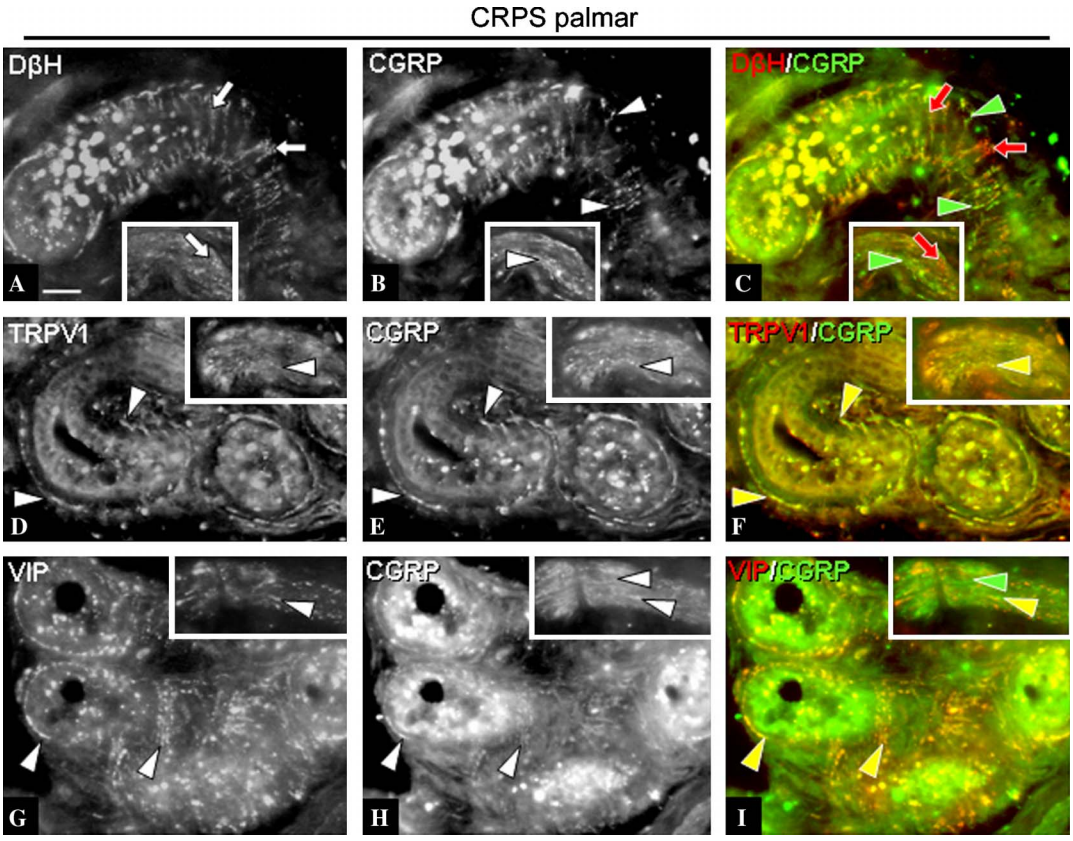

Fig. 9. The innervation on sweat glands located deep in CRPS dermis differed substantially from that of normal sweat glands or CRPS sweat glands located more superficially (i.e., Fig. 8). Small deep nerves located among these sweat glands are shown in the insets. (A–C) The deep sweat glands received a substantial innervation that labeled with DβH and with CGRP (arrows and arrowheads, respectively) that were mostly expressed in separate but intermingled fibers. (D–I) The CGRP component of the deep sweat gland innervation completely co-expressed TRPV1 and VIP. TRPV1 was not normally detected, and VIP normally labels most of the sweat gland innervation without co-expressing CGRP, in control sweat gland innervation. Scale bar = 50 μm.

cussed pertaining to sweat gland function. However, a minor contingent of fibers may normally retain adrenergic properties (Landis, 1999). Also, a component of the sweat gland innervation contains CGRP. Some of the CGRP-positive processes appear to lack VIP and may be sensory in nature, although an origin from sensory neurons has not been directly documented, while other CGRP-positive processes appear to co-express VIP and may be a subset of sympathetic innervation. Our examination indicated that VIP and CGRP can often be detected independently in what appear to be separate but closely intermingled fibers.

PGP labeling revealed that sweat glands in control skin contained dense innervation concentrated around the perimeter of sweat gland tubules, as well as innervation among small blood vessels intermingled among the tubules (Fig. 8A). As seen with other antibodies, sweat glands from control skin had innervation concentrated around the tubules that consistently contained a mix of profiles, most of which labeled for VIP (Fig. 8B) and CGRP (Fig. 8C; Table 2). As is generally seen with most control vasculature, the small blood vessels intermingled among the sweat gland tubules were innervated by NPY-positive sympathetic fibers and CGRP-positive sensory fibers (Figs. 8C and D). NPY has been shown to be consistently co-expressed with TH and DβH, indicating that vascular sympathetic innervation is normally noradrenergic. Importantly, the innervation concentrated around the perimeter of control sweat gland tubules did not label for NPY (Fig. 8D), or for TH or DβH (not shown). In the CRPS affected arm, the distribution of innervation to some sweat glands appeared similar to that in control skin based upon PGP labeling (Figs. 8E, I, and M), although numerous sweat glands from each region were found to be largely uninnervated (data not shown). Among those sweat glands with remaining PGP-positive innervation, the expression of VIP was largely intact (Figs. 8F, J, and N), however, the expression of CGRP was significantly depleted (Figs. 8G, K, and O; Table 2). Importantly, in many instances, sweat glands from CRPS affected arm regions had aberrant NPY-positive innervation concentrated around the perimeter of sweat gland tubules (Figs. 8H, L, and P) which was never observed in control skin. This abnormal NPY innervation also expressed TH and DβH (e.g., Figs. 9A–C). Similar to that observed in upper

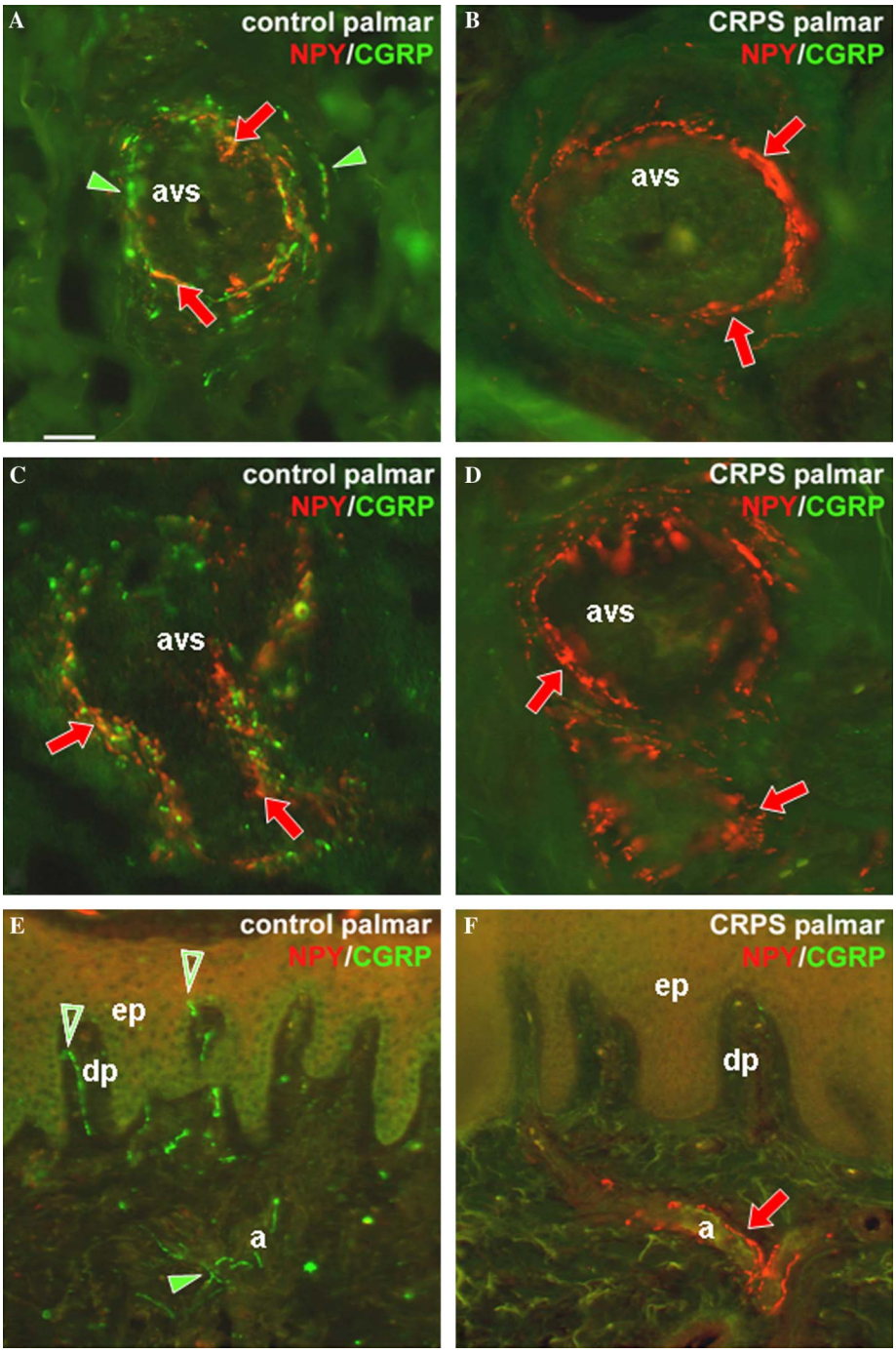

Fig. 10. CRPS palmar skin lacked normal CGRP-positive innervation to vascular components and had aberrant NPY-positive innervation onto superficial arterioles compared with control. (A, C, and E) Control palmar skin contained numerous arteriovenous shunts (avs) in the deep to mid-dermis that were innervated by a mix of NPY-positive (arrows) and CGRP-positive (arrowheads) fibers. The control upper dermis (E) consistently had small arteries or arterioles (a) just below the epidermis (ep) that contained only CGRP-positive fibers (arrowhead). (B, D, and F) In contrast, CRPS affected palmar skin had normal NPY-positive (arrows) innervation to arteriovenous shunts (avs), but had lost the normal expression of CGRP. Additionally, superficial arteries (a) had lost the normal expression of CGRP, but contained an abnormal expression of NPY on innervation (F, arrow). Note the CGRP innervation (open arrowheads) in the dermal papillae (dp) and epidermis of control skin which is lacking in CRPS skin. Scale bar = 25 μm (A–D) and =50 μm (E,F).

extremity skin, many sweat glands in CRPS affected lower extremity regions were completely devoid of PGP-positive innervation (not shown), while among those with remaining innervation, the normal expression of CGRP was also absent, including in those locations that were regarded as uninvolved (Figs. 14B, E, I, L). However, in contrast to the CRPS affected upper extremity, no instances of aberrant NPY-positive inner-

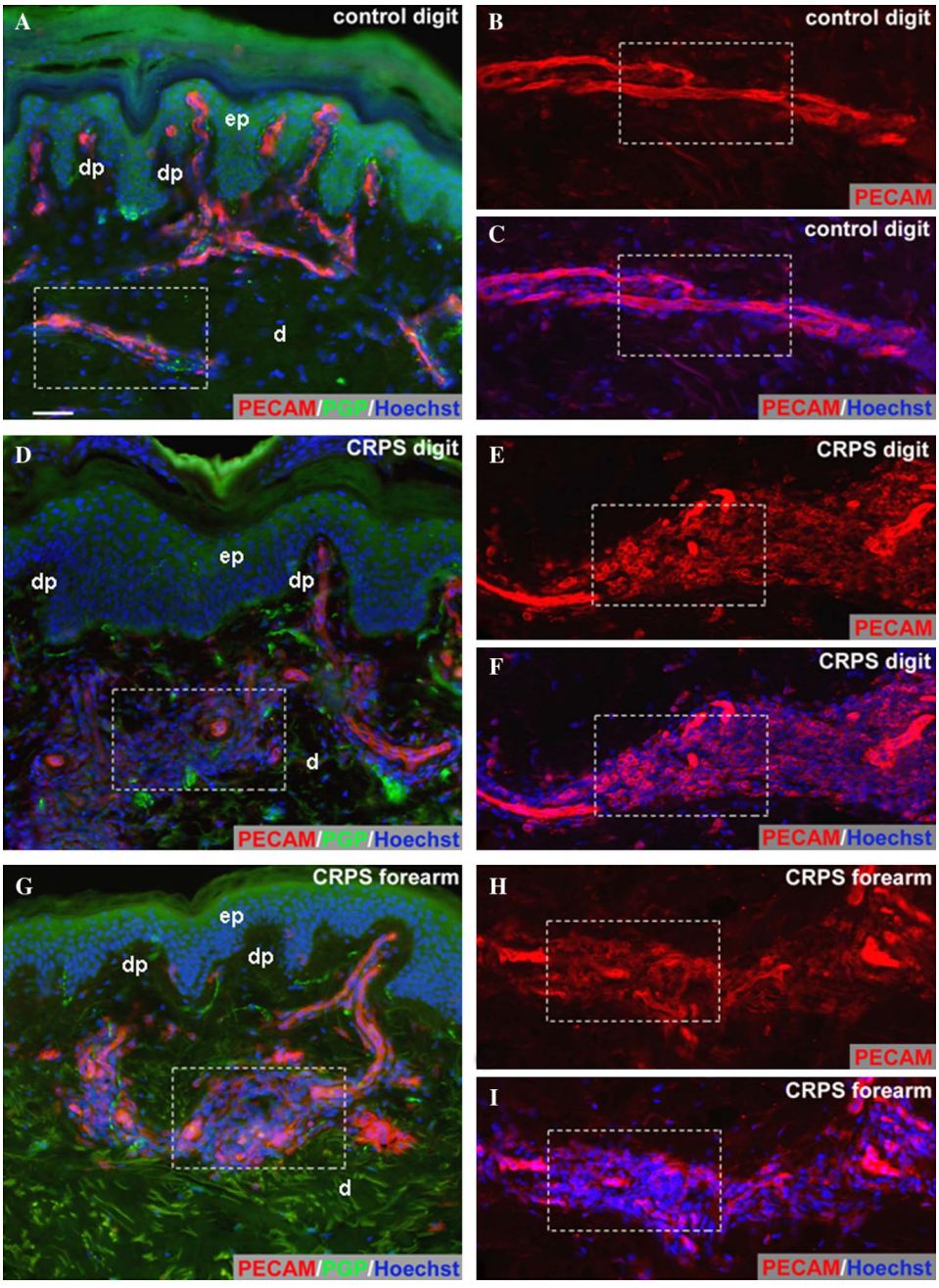

Fig. 11. Regions of CRPS skin had a dramatic loss of vascular integrity and increased perivascular cellular dispersion compared with control. (A–C) Control digit skin had intact, uniform PECAM staining on superficial capillaries and precapillary arterioles (boxes in A and B, respectively), indicative of vascular epithelial integrity. Hoechst staining of cell nuclei demonstrated that the cellular matrix around the vessels was intact (boxes in A and C). Note that all of the dermal papillae in the control skin contained capillaries. (D–I) In contrast, CRPS digit (D, E, and F) and forearm (G, H, and I) skin had a dramatic loss of uniform PECAM staining in superficial capillaries (boxes in D and G) and precapillary arterioles (boxes in E and H), indicative of a loss of superficial capillary integrity. Hoechst staining revealed an increase in cellular dispersion surrounding the disrupted vessels (boxes in D, F, G, and I). Note that a majority of the dispersed cells appear to be PECAM-positive (boxes in F and I), and that many of the dermal papillae lack PECAM labeled capillaries. Scale bar = 50 μm.

vation around the perimeter of sweat gland tubules were observed. Interestingly, some sweat glands in the deep dermis of the CRPS upper extremity had a different combination of aberrant innervation than that more often seen among other CRPS involved sweat glands. In particular, they had the aberrant NPY/TH/DβH-positive innervation (Figs. 9A–C) around the sweat gland tubules, but also had CGRP innervation (Figs. 9D–I). However, this CGRP-positive sweat gland innervation completely co-localized with nearly all of the VIP-positive innervation (Figs. 9D–F) and also co-expressed TRPV1 (Figs. 9G–I). In contrast, control

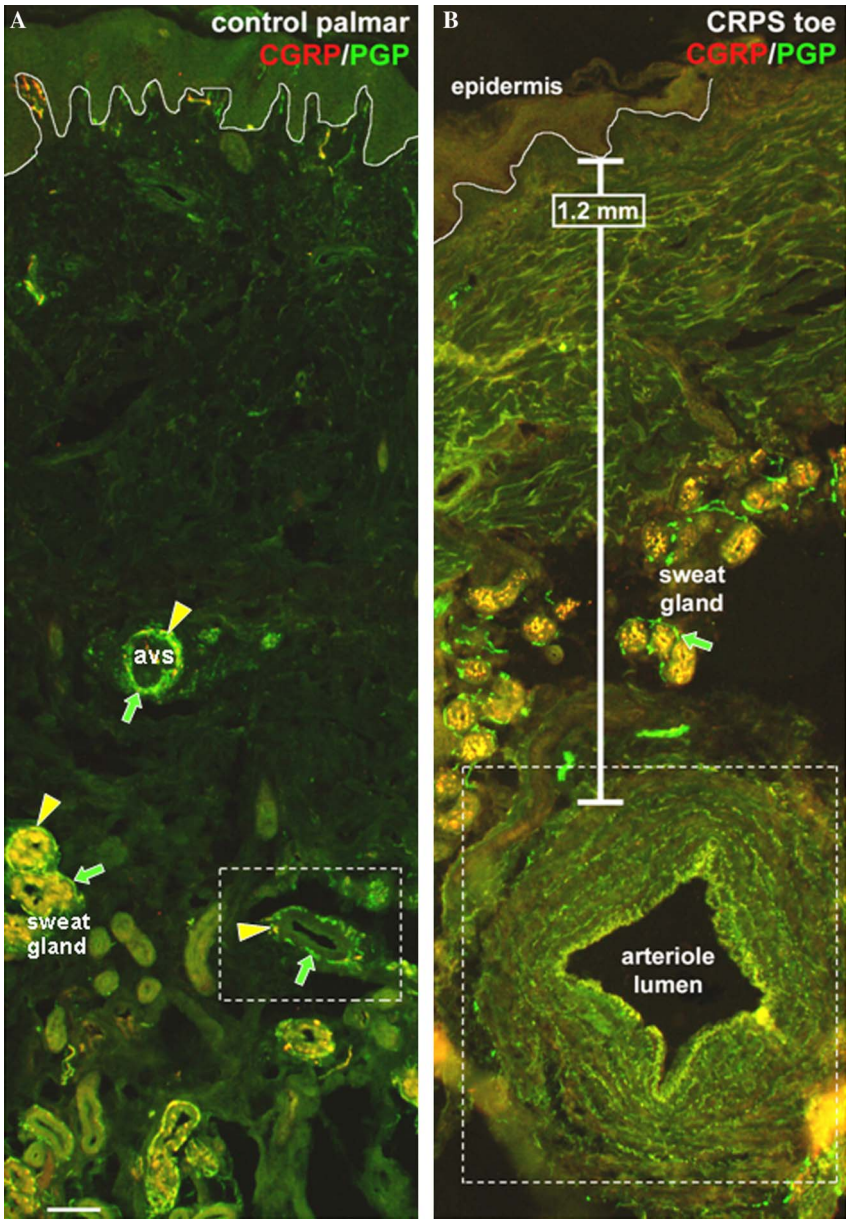

Fig. 12. CRPS affected skin contained presumptive arteries that had lost innervation and had become hypertrophied. (A) Control palmar skin contained sweat glands, arteries (box), and arteriovenous shunts (avs) located within 2 mm of the epidermis (basement membrane delineated by the white line) that all contained abundant PGP-positive innervation (arrows) of which some co-expressed CGRP (arrowheads). (B) In contrast, CRPS affected skin contained sweat glands with some remaining PGP-positive innervation (arrow), of which none expressed CGRP, and denervated arteries (box) that had become extremely hypertrophied with a characteristic pathology of a multi-laminated wall. Scale bar = 100 μM.

CGRP-positive sweat gland innervation lacked TRPV1 and was either a subset of, or separate from, the more extensive VIP-positive innervation.

3.6. Vasculature innervation

Normal cutaneous vascular innervation consists of dense noradrenergic sympathetic innervation concentrated at the tunica media-adventitia border of arteries, arterioles, and arteriovenous shunts (AVS). In addition to TH and DβH involved in the synthesis of vasoconstrictive noradrenalin, this innervation normally contains NPY that may facilitate vasoconstriction at high levels of sympathetic stimulation (Kennedy et al., 1986; Lundberg et al., 1986; Burnstock and Ralevic, 1994). The tunica adventitia of these vessels is also supplied by Aδ fibers (NF-positive/MBP-positive) and C fibers (NF-negative/MBP-negative) that express the vasodilatory peptides, CGRP and SP (Fundin et al., 1997b; Rice and Rasmusson, 2000; Fünfschilling et al., 2004). C fiber peptidergic sensory innervation also terminates on small vessels and capillaries in the upper der-

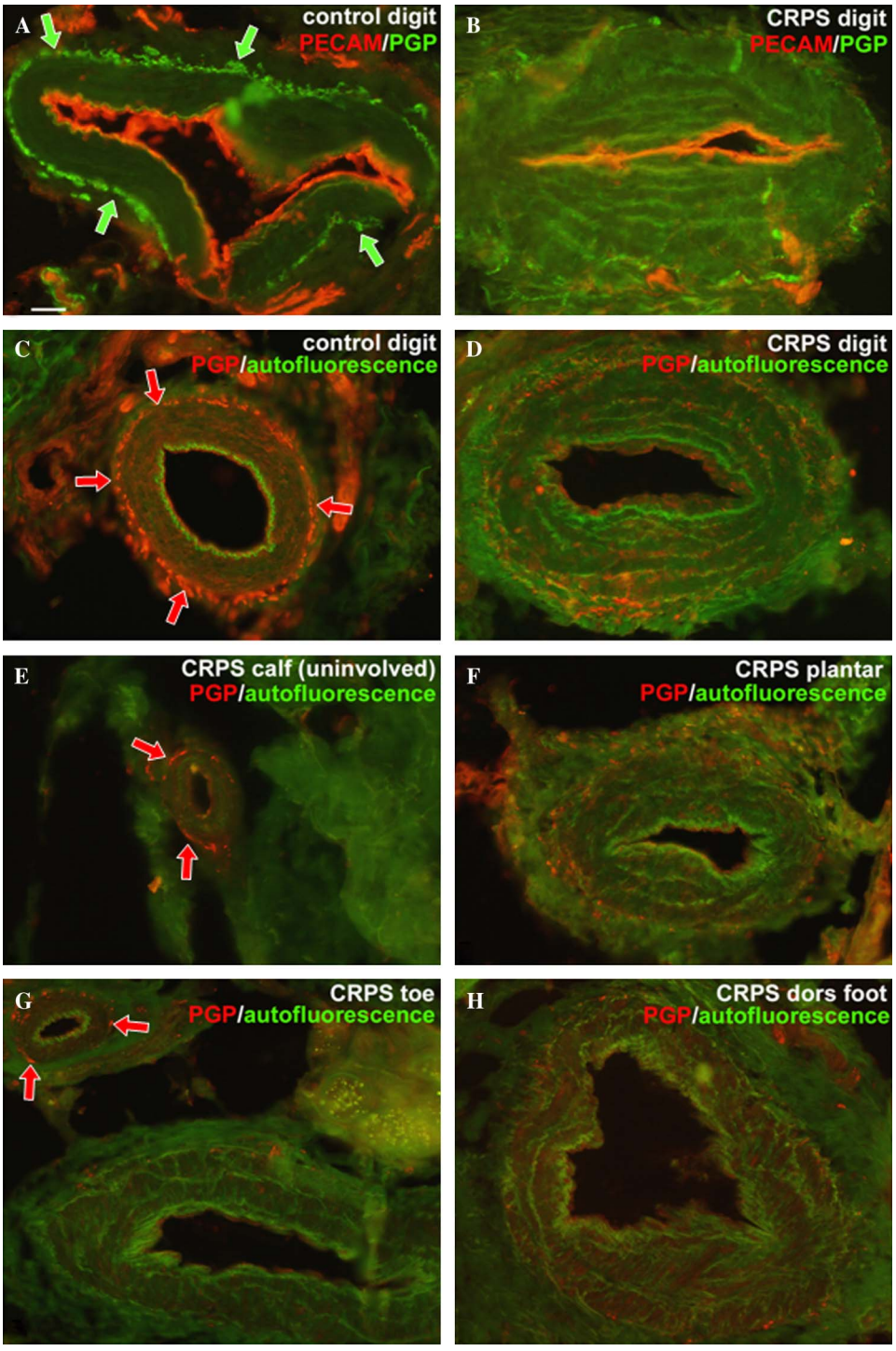

Fig. 13. Regions of CRPS skin had denervated arteries that had become hypertrophied and multi-laminated compared with control or innervated arteries. (A,C) Arteries from control digit skin contained PGP-positive innervation (arrows) around the entire perimeter of the vessel and also had only a single inner band of autofluorescent elastin adjacent to the vessel lumen. (E) As well, arteries from uninvolved CRPS calf skin (E) and select arteries from CRPS toe skin (upper left of G) retained some PGP-positive innervation (arrows in E, G) and single laminar organization. (B, D, F–H) In contrast, CRPS affected skin showed dramatic arterial abnormalities characterized by an overall loss of PGP-positive innervation coupled with hypertrophic, multi-laminated vascular walls. The abnormalities of the artery walls were never found in any region of control skin (A, C) or uninvolved CRPS calf skin (E) and were only a characteristic of denervated vessels from CRPS affected skin (note the differences of the two adjacent vessels in G). Scale bar = 50 μm.

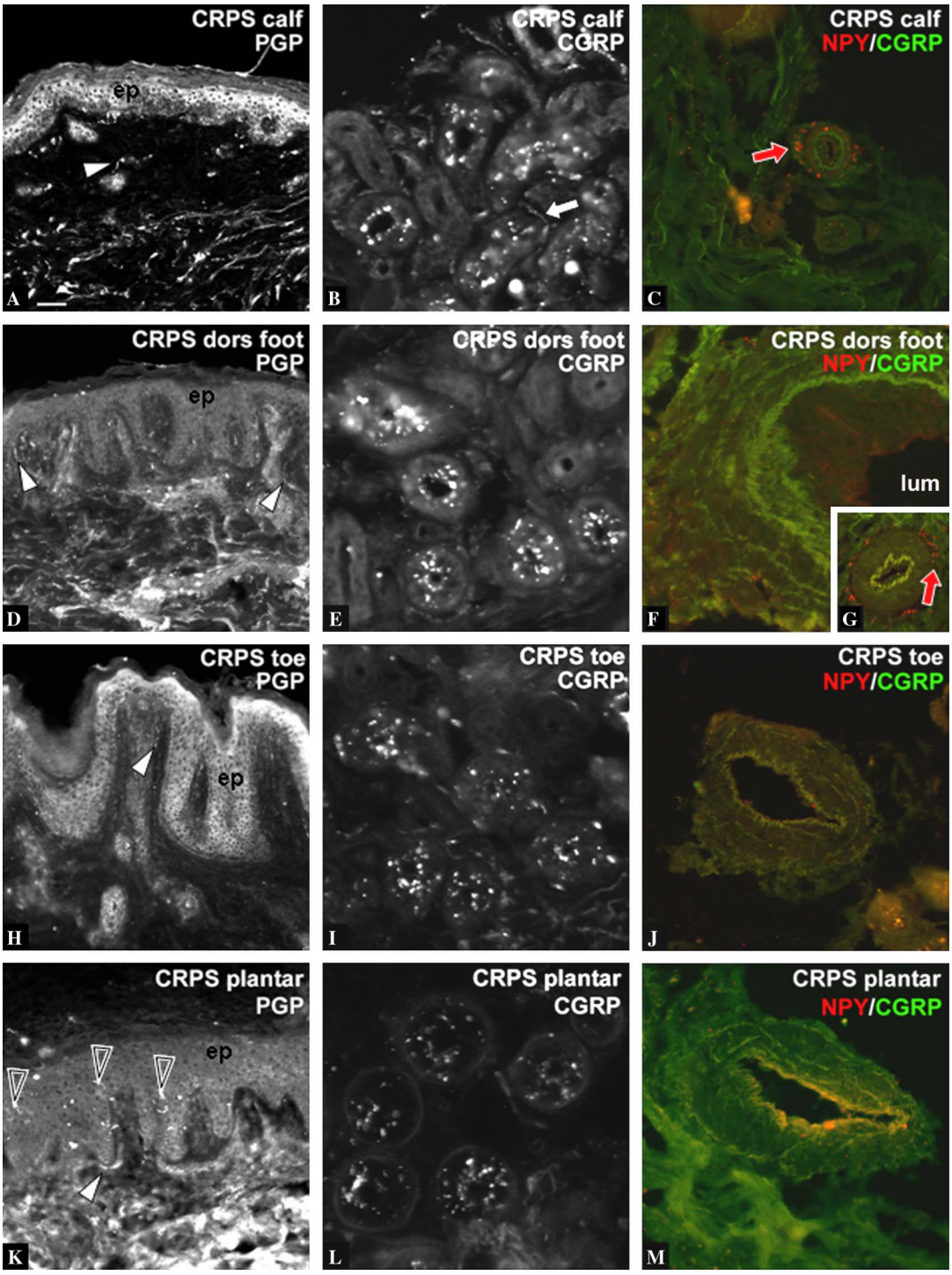

Fig. 14. CRPS affected lower extremity skin regions contained comparable pathologic features as seen in affected upper extremity skin. (A–M) The CRPS affected skin from the lower extremity had a loss of epidermal fibers, a loss of CGRP in sweat gland and artery innervation, and denervated vessels with associated characteristic hypertrophy. Lower extremity calf (A), dorsal foot (D), toe (H), and plantar (K) regions contained very little upper dermal (arrowheads) or epidermal (open arrowheads) innervation. Sweat glands from the calf region (B) retained limited CGRP expression on the remaining innervation (arrow), while sweat glands from the dorsal foot (E), toe (I), and plantar (L) regions were devoid of CGRP labeling. The arteries from the calf region (C) had lost CGRP expression, but retained NPY expression on the remaining innervation (arrow) and were without pathologic multi-laminated, hypertrophic walls. Most arteries from the dorsal foot region (F) that had lost CGRP and NPY expression were hypertrophic and showed the characteristic multi-laminated vessel walls, however some vessels from the same affected region (G), that had also lost the expression of CGRP but retained NPY expression on innervation (arrow), were not hypertrophic and were without pathologic multi-laminated walls. Arteries from CRPS affected toe (J) and plantar (M) regions had also lost the normal expression of CGRP and NPY and showed the characteristic pathology of hypertrophy and multi-laminated vessel walls. Scale bar = 50 μm (A, C, D, F, G, H, J, K, and M); 25 μm (B, E, I, L).

Table 2
Quantification analysis results

Control			CRPS		
Forearm	Palm	Digit	Forearm	Palm	Digit
PGP-positive epidermal endings/mm epidermal length					
6.84 ± 0.12	8.10 ± 0.44	5.40 ± 0.19	2.52 ± 0.48*	0.62 ± 0.17*	1.35 ± 0.19*
CGRP-positive epidermal endings/mm epidermal length					
0.73 ± 0.12	1.15 ± 0.14	1.98 ± 0.17	0.24 ± 0.08^	0.12 ± 0.08*	0.17 ± 0.09*
Control vessels			CRPS vessels		
Forearm	Palm	Digit	Forearm	Palm	Digit
# of vascular and sweat gland profiles with CGRP-positive innervation					
20/20	20/20	20/20	2/20°	0/20°	3/20°
Control sweat glands			CRPS sweat glands		
Forearm	Palm	Digit	Forearm	Palm	Digit
17/20	20/20	18/20	3/20°	6/20°	4/20°

For PGP-positive and CGRP-positive epidermal innervation counts, three random sections each from control and CRPS affected regions were used. Data are presented as means ± SE of the fiber counts/mm epidermis and were compared using Student's *t*-test. For vascular and sweat gland innervation, 20 random profiles each of dermal arteries and sweat glands from each region of control and CRPS affected skin were evaluated for the presence of CGRP-positive fibers. The data are presented as the number of profiles with positive CGRP innervation of the 20 examined and were compared by a two-tailed Fisher's Exact test.

* $p < 0.01$ compared with corresponding control region by Student's *t*-test.

^ $p < 0.05$ compared with corresponding control region by Student's *t*-test.

° $p < 0.001$ compared with corresponding control region by two-tailed Fisher's Exact test.

mis that lack sympathetic innervation (Fundin et al., 1997a,b; Fünfschilling et al., 2004). Various double label combinations have revealed that the only other vascular innervation may be a CGRP-negative Aδ fiber contribution to AVS.

Innervation to the vasculature from control palmar skin (Figs. 10A, C, and E) included mutually exclusive NPY/TH-positive and CGRP/SP-positive fibers on AVS (Fig. 10A), superficial dermal precapillary arterioles (Fig. 10C), and dermal arteries (Table 2). In control palmar skin, all of the innervation to superficial dermal precapillary arterioles labeled with CGRP (Fig. 10E), but never labeled with NPY (Fig. 10E). Innervation to the vasculature from CRPS affected palmar skin (Figs. 10B, D, and F) retained the normal NPY-positive expression, but was devoid of the normal CGRP expression on AVS (Figs. 10B and D). A significant reduction in CGRP-positive dermal artery innervation was detected in CRPS-affected upper extremity regions compared with control (Table 2). As well, superficial precapillary arterioles were devoid of the normal CGRP expression, but did contain abnormal NPY-positive innervation (Fig. 10F). The loss of CGRP expression and gain of abnormal NPY expression on the innervation to the upper dermal arterioles was similar to that seen in the sweat glands.

3.7. Vascular abnormalities

In addition to observing innervation abnormalities on CRPS affected vasculature, pathologic changes of the vessels themselves were also found (Figs. 11–14). Using antibodies directed against the platelet endothelial cell adhesion marker (PECAM), the endothelial lining of the vasculature could be easily visualized. When this was combined with a Hoechst DNA counterstain to visualize cell nuclei, the integrity of the vasculature could be evaluated. Control digit skin (Figs. 11A–C) had an intact superficial network of PECAM-positive arterioles and capillaries (Fig. 11A). The PECAM staining was uniform along the length of the vessels and demonstrated the epithelial cell integrity necessary for normal vascular function (Fig. 11B). The combination with the Hoechst counterstain further demonstrated the normal, intact cellular matrix around the vessels (Figs. 11A and C). In contrast, CRPS affected digit skin (Figs. 11D–F) had lost the normal uniform PECAM staining indicative of superficial arteriole and capillary integrity (Figs. 11D and E). Combination with the Hoechst counterstain revealed a drastic increase in cellular dispersion around the disrupted vessels (Figs. 11D and F). Similarly, in CRPS affected forearm skin (Figs. 11G–I) superficial arterioles and capillaries had lost the normal uniform PECAM staining indicative of vascular integrity (Figs. 11G and H) and had a drastic increase in cellular dispersion around the disrupted vessels (Fig. 11G). Interestingly, the majority of the dispersed cells at the vascular interface appear to be PECAM-positive (Figs. 11E, F, H, and I), indicating the probability that the vascular endothelium had disrupted cellular adhesion properties.

Control vasculature in superficial locations had robust innervation, maintained a single laminated vessel wall, and retained a size that was appropriate for the location/function of the vessel. Conversely, CRPS affected skin contained numerous denervated vessels that had become extremely hypertrophied, characterized by an increase in the overall vessel diameter, an increase in the size of the lumen, and a thickened multi-laminated wall. For example, control palmar skin has ample PGP-positive/CGRP-positive innervation to AVS, sweat glands, and arteries (Fig. 12A), all located within ~1.5 mm of the epidermis. CRPS affected skin had some remaining PGP-positive, but CGRP-negative, innervation to sweat glands, with very limited, if any, innervation onto vessels located in a similarly superficial location (Fig. 12B). Furthermore, the denervated vessels from CRPS affected skin had a dramatic hypertrophic profile, characterized by the appearance of a multi-laminated vascular wall (Fig. 12B), compared with innervated control vessels (Fig. 12A).

Control digit skin contained large arteries that had robust PECAM labeling of the endothelial wall and PGP-positive innervation around the entire vessel (Figs. 13A and C). Despite the size of some of the control arteries, they always appeared as single laminated vessels with a single inner band of autofluorescent elastin (Fig. 13C). CRPS affected digit skin (Figs. 13B and D), which also had good PECAM staining of the endothelial cells (Fig. 13B), lacked any appreciable PGP-positive innervation, and the denervated vessels were extremely hypertrophied with multi-laminated vessel walls and the appearance of multiple autofluorescent elastin-like bands (Figs. 13B and D). Skin from the CRPS uninvolved (non-painful) calf region retained relatively normal PGP-positive innervation to the arteries, and they appeared as single laminated vessels with only a single inner band of autofluorescent elastin (Fig. 13E). In contrast, the uninvolved (non-painful) skin from the glabrous plantar foot (Fig. 13F), as well as the involved (painful) skin from the dorsal toe (Fig. 13G) and dorsal foot (Fig. 13H), contained numerous vessels devoid of PGP-positive innervation that were extremely hypertrophied with multi-laminated vessel walls and the appearance of multiple autofluorescent elastin-like bands (Figs. 13F–H). Importantly, note the distinct difference in the two vessels depicted in Fig. 13G. The vessel in the top left corner retained PGP-positive innervation and a normal appearing single laminated vessel wall and single inner band of autofluorescent elastin, whereas the adjacent vessel was devoid of PGP-positive innervation and had become hypertrophied with the appearance of a multi-laminated vessel wall and multiple autofluorescent elastin-like bands. Furthermore, the lower extremity vessels that were devoid of PGP-positive innervation and had become hypertrophied with multi-laminated vessel walls,were also devoid of CGRP and NPY expression (Figs. 14F, J, M), implying that neuronal innervation to these vessels was indeed lost and not that PGP expression was downregulated. Additionally, similar to that observed in CRPS affected upper extremity skin (see Fig. 10), CRPS lower extremity skin vessels from calf and other leg regions that retained PGP-positive innervation and a normal appearance had also lost the normal expression of CGRP while retaining the expression of NPY (Figs. 14C and G).

4. Discussion

CRPS type I is a multi-faceted, multi-system affliction with a diverse etiology and an unknown pathologic mechanism. The broadly defined clinical criteria include disturbances of the somatosensory, autonomic, and motor systems (Galer et al., 2001; Raja and Grabow, 2002; Kirkpatrick, 2003), and clinical diagnosis of CRPS I, by definition, is not associated with a defined nerve lesion. Although previous work with CRPS affected tissues found several anomalies in muscle and bone structure, very little has been shown in the way of nerve pathology (Basle et al., 1983; van der Laan et al., 1998). Here, the severity of pain and general health of the limb in two advanced CRPS I patients ultimately necessitated amputation as a last resort. In contrast to skin assessments afforded by more limited 3 mm punch biopsies (Drummond et al., 1996), these amputations provided extensive skin samples that demonstrated several profound changes in cutaneous innervation and vasculature of the affected skin as compared with skin from similar upper extremity regions from normal volunteers, non-painful lower extremity skin sites from the same patient, and normal skin from other species including monkeys (Fundin et al., 1997a,b; Rice et al., 1997; Rice and Rasmusson, 2000; Paré et al., 2001, 2002, 2003; Petersen et al., 2002; Fünfschilling et al., 2004).

4.1. Nerve and sensory innervation pathologies

As seen in control human skin and in skin from normal rodents, carnivores, and monkeys, cutaneous nerves typically contain a mixture of thick and thin caliber NF-positive axons that most always co-express MBP, indicating that they are likely Aβ and Aδ fibers, respectively (Fundin et al., 1997a; Rice et al., 1997; Rice and Rasmusson, 2000; Paré et al., 2001, 2002). In contrast to normal nerves, nerves from the CRPS skin had some thick caliber myelinated axons, but also contained an abnormally high proportion of densely packed thin caliber NF-positive axons that lacked MBP. The nerves lacked intervening gaps normally filled by NF-negative C fibers and had few fibers that expressed CGRP or SP. These observations indicate that the CRPS involved nerves had a substantial loss of normal C and Aδ fibers, and contained numerous aberrant axons of unknown

origin, and presumably, altered function. These fibers may have been sprouted Aβ fibers that failed to innervate a proper target and achieve a caliber size that induced myelination (Voyvodic, 1989), or they may have been demyelinated Aδ fibers, or C fibers that upregulated NF. Recent work from our laboratory indicates that many, if not most, C fibers normally express GAP43, which is lacking in normal Aβ or Aδ fibers. This suggests that C fiber endings may be constantly remodeling, whereas the Aβ and Aδ-fiber endings are relatively stable. The thin-caliber NF-positive, but unmyelinated, axons in the CRPS nerves generally lack GAP43, suggesting that their aberrant terminations, described below, may also be relatively stable.

Importantly, scattered locations within the relatively denervated epidermis of CRPS skin had remaining endings that had highly branched, widespread arbors in the epidermis instead of a normal relatively unbranched, radially oriented morphology. Some foci in the upper dermis had aberrant clusters of NF-positive profiles accompanied by endings penetrating into the epidermis that were also NF-positive. The scattered clusters of NF-positive innervation in the upper dermis and epidermis may be terminations of the aberrant unmyelinated thin-caliber NF-positive axons observed in the nerves. Normal NF-positive innervation to the upper dermis is either organized into morphologically distinct Aβ-fiber Merkel or Meissner corpuscles, or consists of relative sparse, radially oriented Aδ-fibers that lose detectable NF as their endings penetrate the epidermis. Similar aberrantly branched endings with abnormal immunochemical characteristics have also been observed in a patient with severe postherpetic neuralgia (Petersen et al., 2002) and might be hypothesized irritable nociceptors (Fields et al., 1998).

In addition, CRPS affected skin contained numerous ectopic dense plexuses of similar small caliber, NF-positive, but unmyelinated, fibers concentrated around hair follicles below the level where Aβ and C-fibers normally terminate as highly organized piloneural complexes, and the piloneural complexes in CRPS hair follicles were in disarray. This type of abnormal and disarrayed innervation around hair follicles may account for the severe allodynia commonly observed in CRPS patients upon slight hair deflection. Likewise, aberrant tangles of NF-positive fibers were seen to supplant the normal Meissner corpuscle in dermal papilla of CRPS skin, and these fibers may account for the painful conditions in affected glabrous skin.

4.2. Sweat gland pathology

Among the sweat glands in CRPS skin, many appeared to be denervated, whereas in others, the remaining innervation retained VIP expression, but lost CGRP expression, suggesting that only presumptive sensory innervation had been lost. In some instances, the expression of NPY appears on the innervation to sweat glands in CRPS skin, accompanied by higher than normal levels of TH and DβH, suggesting that adrenergic sympathetic fibers may have sprouted from innervation on blood vessels contained within the glands or that existing sympathetic innervation may have re-expressed adrenergic properties.

Interestingly, deep sweat glands were virtually the only target in the CRPS skin where CGRP-positive innervation persisted. As noted above, CGRP-positive fibers were nearly absent in nerves and targets located more superficially. However, CGRP-positive fibers were present in the nerves within the deep dermis, suggesting that some of these are the source of the CGRP innervation to the deep sweat glands. Importantly, this CGRP-positive innervation to sweat glands also co-expressed TRPV1 which is not normally present among sweat gland innervation. Normally, TRPV1-positive innervation is found on a subset of CGRP-negative innervation in the epidermis or on a subset of CGRP-positive innervation to blood vessels (Molliver et al., 2005; Paré et al., 2001; Petersen et al., 2002). However, in the CRPS skin we did not detect TRPV1 in locations that would normally contain TRPV1-positive innervation. Therefore, the presence of TRPV1 on CGRP innervation in the deep sweat glands may be due to an abnormal de novo expression of TRPV1 on remaining sweat gland innervation, or abnormal sprouting and targeting of presumptive TRPV1/CGRP-positive vascular innervation onto the sweat glands. Overall, these observed aberrations present among CRPS sweat gland innervation likely contributed to the autonomic dysfunction seen in these patients with CRPS.

4.3. Vascular pathology

In these CRPS patients, CGRP-positive innervation was significantly decreased among all the vascular innervation compared with control skin. These findings contrast with several reports of increased neurogenic inflammation and CGRP plasma content of acutely affected, and previously unaffected contralateral limbs of CRPS patients, indicating a likely increase in CGRP or receptor levels (Blair et al., 1998; Weber et al., 2001; Leis et al., 2003). However, the data presented here are from chronic CRPS patients and may be indicative of the further manifestation of the ongoing disorder. Acute CRPS changes may result in an increased neurogenic inflammatory response and increases in CGRP or CGRP receptors, but as the disorder progresses the CGRP-positive fibers innervating the vasculature may be lost. Double label combinations with antibodies against CGRP, NF, NPY, and PGP indicated that CGRP levels were not merely depleted, but that most of the sensory innervation was missing in the tunica adv-

entia of arteries, arterioles, and AVS. While most of the innervation among upper dermal vessels was also missing, remaining fibers lacked CGRP, and some abnormally expressed NPY. This may have been due to downregulation of CGRP and upregulation of NPY in extant sensory fibers, or potential ectopic sprouting of sympathetic innervation.

Although sensory peptidergic innervation seemed generally lacking among arterial components, considerable variability existed among sympathetic innervation. Some arteries contained normal appearing sympathetic innervation, whereas neighboring arteries within the same section lacked all sensory and sympathetic innervation. The denervated dermal vessels, often less than 2 mm below the epidermis, had gross hypertrophic changes consisting of a thickened multi-laminar wall and enlarged lumen. A similar vessel pathology has been previously reported in muscle and bone tissue from CRPS affected patients (Basle et al., 1983; van der Laan et al., 1998). This peculiar pathology may likely represent a direct vascular tissue response to the loss of sympathetic-regulated muscular tone. Furthermore, the resultant distortion of the surrounding tissue as a consequence of the hypertrophic vessels may contribute to the sensation of intractable, deep aching, constant pain often observed as a clinical symptom in CRPS patients.

5. Conclusions

This study was limited to only two CRPS type I patients, and we did not have equally extensive control tissue. However, the histopathologic changes that we report are clear deviations from normal innervation and structure that we have seen in control skin tissue from human, monkey, and a wide variety of other mammals. Amputation is reserved as a final option for intractable pain patients and was performed in these cases only after exhaustive attempts at conventional therapies failed and the affected limbs became a general health issue for each patient. As such, we cannot rule out the possibility that the observed changes in these skin samples were attributable to the various treatment regimen attempted prior to amputation, as opposed to the disease itself.

Importantly, though, our results demonstrate numerous abnormal changes in cutaneous innervation and in vascular innervation and structure. These deviations confirm that, at least in some cases, CRPS type I can be associated with peripheral neuropathic conditions consistent with the myriad of observed clinical symptoms (van der Laan et al., 1998).

Acknowledgments

The authors thank Mrs. Jenny Dye and the RSD Awareness Coalition for financial contributions toward this research. We thank Marilyn Dockum and Avishkar Tyagi for assistance with tissue processing, and Dr. David J. Schreyer and Dr. Laura S. Stone for gifts of antibodies. This work is dedicated to several friends suffering with CRPS.

References

Basle MF, Rebel A, Renier JC. Bone tissue in reflex sympathetic dystrophy syndrome–Sudeck's atrophy: structural and ultrastructural studies. Metab Bone Dis Relat Res 1983;4:305–11.

Blair SJ, Chinthagada M, Hoppenstehdt D, Kijowski R, Fareed J. Role of neuropeptides in pathogenesis of reflex sympathetic dystrophy. Acta Orthop Belg 1998;64:448–51.

Burnstock G, Ralevic V. New insights into the local regulation of blood flow by perivascular nerves and endothelium. Br J Plast Surg 1994;47:527–43.

Drummond PD, Finch PM, Gibbins I. Innervation of hyperalgesic skin in patients with complex regional pain syndrome. Clin J Pain 1996;12:222–31.

Drummond PD, Finch PM, Smythe GA. Reflex sympathetic dystrophy: the significance of differing plasma catecholamine concentrations in affected and unaffected limbs. Brain 1991;114(Pt 5):2025–36.

Eisenberg E, Chistyakov AV, Yudashkin M, Kaplan B, Hafner H, Feinsod M. Evidence for cortical hyperexcitability of the affected limb representation area in CRPS: a psychophysical and transcranial magnetic stimulation study. Pain 2005;113:99–105.

Fields HL, Rowbotham M, Baron R. Postherpetic neuralgia: irritable nociceptors and deafferentation. Neurobiol Dis 1998;5:209–27.

Fundin BT, Arvidsson J, Aldskogius H, Johansson O, Rice SN, Rice FL. Comprehensive immunofluorescence and lectin binding analysis of intervibrissal fur innervation in the mystacial pad of the rat. J Comp Neurol 1997a;385:185–206.

Fundin BT, Pfaller K, Rice FL. Different distributions of the sensory and autonomic innervation among the microvasculature of the rat mystacial pad. J Comp Neurol 1997b;389:545–68.

Fünfschilling U, Ng YG, Zang K, Miyazaki J, Reichardt LF, Rice FL. TrkC kinase expression in distinct subsets of cutaneous trigeminal innervation and nonneuronal cells. J Comp Neurol 2004;480:392–414.

Galer B, Schwartz L, Allen R. complex regional pain syndromes – type i: reflex sympathetic dystrophy, and type II: Causalgia. In: Loeser J, editor. Bonica's Management of Pain. Philadelphia: Lippencott, Williams & Williams; 2001. p. 388–411.

Harden RN, Duc TA, Williams TR, Coley D, Cate JC, Gracely RH. Norepinephrine and epinephrine levels in affected versus unaffected limbs in sympathetically maintained pain. Clin J Pain 1994;10:324–30.

Holland NR, Stocks A, Hauer P, Cornblath DR, Griffin JW, McArthur JC. Intraepidermal nerve fiber density in patients with painful sensory neuropathy. Neurology 1997;48:708–11.

Jänig W. The sympathetic nervous system in pain: physiology and pathophysiology. In: Stanton-Hicks M, editor. Pain and the Sympathetic Nervous System. Boston: Kluwer Academic; 1990. p. 17–89.

Jänig W, Baron R. Complex regional pain syndrome: mystery explained? Lancet Neurol 2003;2:687–97.

Kennedy C, Saville VL, Burnstock G. The contributions of noradrenaline and ATP to the responses of the rabbit central ear artery to sympathetic nerve stimulation depend on the parameters of stimulation. Eur J Pharmacol 1986;122:291–300.

Kirkpatrick, A., Reflex Sympathetic Dystrophy/Complex Regional Pain Syndrome (RSD/CRPS): Clinical Practice Guidelines – 3rd ed., in: A. Kirkpatrick (Ed.), Vol. 2004, International RSD Foundation, 2003.

Landis SC. Development of muscarinic receptors and regulation of secretory responsiveness in rodent sweat glands. Life Sci 1999;64:381–5.

Leis S, Weber M, Isselmann A, Schmelz M, Birklein F. Substance-P-induced protein extravasation is bilaterally increased in complex regional pain syndrome. Exp Neurol 2003;183:197–204.

Lundberg JM, Rudehill A, Sollevi A, Theodorsson-Norheim E, Hamberger B. Frequency- and reserpine-dependent chemical coding of sympathetic transmission: differential release of noradrenaline and neuropeptide Y from pig spleen. Neurosci Lett 1986;63:96–100.

Molliver DC, Immke DC, Fierro L, Pare M, Rice FL, McCleskey EW. ASIC3, an acid-sensing ion channel, is expressed in metaboreceptive sensory neurons. Mol Pain 2005;1:35.

Oaklander AL. The density of remaining nerve endings in human skin with and without postherpetic neuralgia after shingles. Pain 2001;92:139–45.

Paré M, Behets C, Cornu O. Paucity of presumptive ruffini corpuscles in the index finger pad of humans. J Comp Neurol 2003;456:260–6.

Paré M, Elde R, Mazurkiewicz JE, Smith AM, Rice FL. The Meissner corpuscle revised: a multiafferented mechanoreceptor with nociceptor immunochemical properties. J Neurosci 2001;21:7236–346.

Paré M, Smith AM, Rice FL. Distribution and terminal arborizations of cutaneous mechanoreceptors in the glabrous finger pads of the monkey. J Comp Neurol 2002;445:347–59.

Petersen KL, Rice FL, Suess F, Berro M, Rowbotham MC. Relief of post-herpetic neuralgia by surgical removal of painful skin. Pain 2002;98:119–26.

Raja SN, Grabow TS. Complex regional pain syndrome I (reflex sympathetic dystrophy). Anesthesiology 2002;96:1254–60.

Rho RH, Brewer RP, Lamer TJ, Wilson PR. Complex regional pain syndrome. Mayo Clin Proc 2002;77:174–80.

Rice FL, Fundin BT, Arvidsson J, Aldskogius H, Johansson O. Comprehensive immunofluorescence and lectin binding analysis of vibrissal follicle sinus complex innervation in the mystacial pad of the rat. J Comp Neurol 1997;385:149–84.

Rice FL, Rasmusson DD. Innervation of the digit on the forepaw of the raccoon. J Comp Neurol 2000;417:467–90.

Rowbotham MC, Fields HL. The relationship of pain, allodynia and thermal sensation in post-herpetic neuralgia. Brain 1996;119(Pt 2):347–54.

Sato J, Perl ER. Adrenergic excitation of cutaneous pain receptors induced by peripheral nerve injury. Science 1991;251:1608–10.

Schotzinger RJ, Landis SC. Acquisition of cholinergic and peptidergic properties by sympathetic innervation of rat sweat glands requires interaction with normal target. Neuron 1990;5:91–100.

Schwartzman RJ, Popescu A. Reflex sympathetic dystrophy. Curr Rheumatol Rep 2002;4:165–9.

Stanton-Hicks M. Complex regional pain syndrome. Anesthesiol Clin North America 2003;21:733–44.

Stanton-Hicks M, Janig W, Hassenbusch S, Haddox JD, Boas R, Wilson P. Reflex sympathetic dystrophy: changing concepts and taxonomy. Pain 1995;63:127–33.

Stone LS, Broberger C, Vulchanova L, Wilcox GL, Hokfelt T, Riedl MS, Elde R. Differential distribution of alpha2A and alpha2C adrenergic receptor immunoreactivity in the rat spinal cord. J Neurosci 1998;18(15):5928–37.

van der Laan L, ter Laak HJ, Gabreels-Festen A, Gabreels F, Goris RJ. Complex regional pain syndrome type I (RSD): pathology of skeletal muscle and peripheral nerve. Neurology 1998;51:20–5.

Voyvodic JT. Target size regulates calibre and myelination of sympathetic axons. Nature 1989;342:430–3.

Wasner G, Backonja MM, Baron R. Traumatic neuralgias: complex regional pain syndromes (reflex sympathetic dystrophy and causalgia): clinical characteristics, pathophysiological mechanisms and therapy. Neurol Clin 1998;16:851–68.

Weber M, Birklein F, Neundorfer B, Schmelz M. Facilitated neurogenic inflammation in complex regional pain syndrome. Pain 2001;91:251–7.